COMPOSITE ASYMPTOTIC MODELS FOR A THIN ELASTIC PLATE

PhD Dissertation

Melike PALSÜ

Eskişehir, 2020

COMPOSITE ASYMPTOTIC MODELS FOR A THIN ELASTIC PLATE

MELİKE PALSÜ

PhD DISSERTATION

Department of Mathematics
Supervisor: Prof. Dr. Barış ERBAŞ

Eskişehir
Eskişehir Technical University
Institute of Graduate Programs
January, 2020

JÜRİ VE ENSTİTÜ ONAYI
(APPROVAL OF JURY AND INSTITUTE)

Melike PALSÜ'nün "**Composite Asymptotic Models for a Thin Elastic Plate**" başlıklı tezi 13/01/2020 tarihinde, aşağıdaki juri tarafından değerlendirilerek "Eskişehir Teknik Üniversitesi Lisansüstü Eğitim-Öğretim ve Sınav Yönetmeliği"nin ilgili maddeleri uyarınca, **Matematik** Anabilim dalında Doktora tezi olarak kabul edilmiştir.

	Ünvanı-Adı Soyadı	İmza
Üye (Tez Danışmanı)	: Prof. Dr. Barış ERBAŞ	.....
Üye	:Prof. Dr. Julius KAPLUNOV	.....
Üye	: Prof. Dr. Sinan ÖZEREN	.....
Üye	: Prof. Dr. Nihal EGE	.....
Üye	: Dr. Öğr. Üyesi Kıvanç TAŞKIN	.....

.....

Enstitü Müdürü

Prof. Dr. Murat TANIŞLI

ABSTRACT

COMPOSITE ASYMPTOTIC MODELS FOR A THIN ELASTIC PLATE

Melike PALSÜ

Department of Mathematics

Eskişehir Technical University, Institute of Graduate Programs, January, 2020

Supervisor: Prof. Dr. Barış ERBAŞ

This thesis is on the dynamic bending and plate extension problems of a thin elastic plate under a given external load. The motivation in the choice of the subject has been the modern industrial applications and particularly the desire to contribute to the approximate analytical solutions, which is believed to be lacking. The exact mathematical formulation as well as the solutions to these models for the problems mentioned above may be quite costly. Therefore a composite asymptotic approach used for the problems in the thesis. On using this method, we considered the dynamic response of the thin elastic plate, more specifically, the asymptotic of the first asymmetric bending mode of the plate. The results/solutions, contrary to the ones existing in literature, in terms of elementary functions and therefore considerably simplified the physical and mathematical analysis of the problem.

Keywords: thin elastic plate, Rayleigh-Lamb equation, dynamic bending, plate extension, antisymmetric modes, symmetric modes, asymptotic model.

ÖZET

İNCE ELASTİK BİR PLAKA İÇİN KOMPOZİT ASİMPTOTİK MODELLER

Melike PALSÜ

Matematik Anabilim Dalı

Eskişehir Teknik Üniversitesi, Lisansüstü Eğitim Enstitüsü, Ocak, 2020

Danışman: Prof. Dr. Barış ERBAŞ

Bu tez, verilen bir dış yük altında ince elastik bir plakanın dinamik eğilmesi ve genişlemesi problemleri üzerinedir. Konunun seçimindeki motivasyon, modern endüstriyel uygulamalar ve özellikle eksik olduğuna inanılan yaklaşık analitik çözümlere katkıda bulunma isteği olmuştur. Kesin matematiksel formülasyonun yanı sıra, pratikte belirtilen sorunlara yönelik çözümler de oldukça maliyetli olabilir. Bu nedenle, tezde ele alınan problemler için kompozit asimptotik yaklaşım kullanılmıştır. Bu yöntem kullanılırken, ince elastik plakanın, başlangıçta plakanın ilk antisimetrik bükme modunun dinamik tepkisi dikkate alınmıştır. Tezde elde edilen sonuçlar/çözümler, literatürde mevcut olanların aksine elemanter fonksiyonlar cinsinden olduğundan, problemin fiziksel ve matematiksel analizini büyük ölçüde basitleştirmiştir.

Anahtar Sözcükler: ince elastik plaka, Rayleigh-Lamb denklemi, dinamik bükülme, plaka genişlemesi, antisimetrik modlar, simetrik modlar, asimptotik model.

For my dad.

ACKNOWLEDGMENTS

I would like to express my eternal gratitude to my supervisor Prof. Dr. Barış ERBAŞ for his guidance and support from my undergraduate to PhD study and research. He has a hand in everything I learn about academic life. I would also like to thank him for introducing me to these subjects when i was just an undergraduate student and encouraging me to study them. In addition to my supervisor, I am grateful to Prof. Dr. Nihal EGE for her support throughout my PhD.

I am also very glad and thankful for having met and worked with Prof. Dr. Julius KAPLUNOV, for his constructive suggestions and his support in all stages of my reseach.

I am very greateful for Prof. Dr. Levent ERASLAN and SODIGEM Team for their support and understanding during my thesis writing process. I would like to thank Cennet KARA for her artistic touches on my work and and also Göktuğ ÖNER for his great last moment helps.

Finally, I would like to thank my mother and grandmother for their love and every kind of support they provided throughout my life.

Melike PALSÜ

January, 2020

13/01/2020

STATEMENT OF COMPLIANCE WITH ETHICAL PRINCIPLES AND RULES

I hereby truthfully declare that this thesis is an original work prepared by me; that I have behaved in accordance with the scientific ethical principles and rules throughout the stages of preparation, data collection, analysis and presentation of my work; that I have cited the sources of all the data and information that could be obtained within the scope of this study, and included these sources in the references section; and that this study has been scanned for plagiarism with "scientific plagiarism detection program" used by Eskişehir Technical University, and that "it does not have any plagiarism" whatsoever. I also declare that, if a case contrary to my declaration is detected in my work at any time, I hereby express my consent to all the ethical and legal consequences that are involved.

Melike PALSÜ

TABLE OF CONTENTS

Page

Page

LIST OF FIGURES

Page

Page

LIST OF ABBREVIATIONS

Δ : Laplace's Operator

∇ : Gradient vector field

σ_{ij} : Components of stress

λ,μ : Lame constants

E : Young's modulus

ν : Poisson's ratio

c_1 : Longitudinal wave speed

c_2 : Transverse wave speed

c_R : Rayleigh wave speed

ϕ, ψ : Wave potentials

$\sqrt{-\Delta}$: Pseuodo-differential operator

1. INTRODUCTION

The classical theory of plates and shells, which include the relations of forces, displacements, stresses and strains in an elastic structure, is one of the important areas of mathematical theory of elasticity. The first mathematical approach to the membrane theory of thin plates was formulated by L. Euler in 1766, dealing with free vibration analysis of plate problems [1]. In 1890 Kirchhoff published an important thesis on thin plate theory [2], in which he expressed two independent assumptions, accepted in the theory of plate bending and known as "Kirchoff hypothesis". Other important contributions made by Kirchoff were the obtaining of the frequency equations of plate and introducing the virtual displacement methods in the solution of plate problems. Russian scientists first made great contributions to the architecture of marine vehicles, using solid mathematical theories instead of old trade traditions. Especially Krylov [3] and his student Bubnov [4] made important contributions to the theory of bending and bending-resistant thin plates. Also Timoshenko made important contributions to the theory and practice of plate bending analysis. Timoshenko and Woinowsky-Krieger published a fundamental monograph which contains profound analysis of various plate problems [5].

Scientists such as Hencky [6], Huber [7], von Karman [8]- [9], Nadai [10], Föppl [11] undertook comprehensive studies in the field of plate bending theory of thin plates. Hencky dealt with different types of singularities occurring on plates under point loads, point support effects, etc.

The devolopment of modern aircraft industry has accelerated the analytical analysis of plate problems. Plates under strain and plates which are subjected to plane forces, their behaviour after bending and vibration problems have been analysed by many scientists and engineers. Detailed analyses of thin layers with different geometries, linear and nonlinear bending under different loads and critical loads and forces were considered by Timoshenko and Gere [12], Volmir [13] and Cox [14].

The exact solutions of aforementioned problems require a very special symmetry of correspoding equations and boundary conditions, and in case of real life problems they are quite exceptional. Despite extensive and advanced numerical methods, exact solutions are still the desired ones. Unlike numerical analyses, ap-

proximate asymptotic solutions predict weak or strong asymmetry in the system and can be generalised universally. Asymptotical methods allow the decomposition of equations and thus the geometry of the problem can be understood easily. The construction of approximate theories of thin-walled structures has been the subject of many publications (see [15], [16], [17], [18]). The majority of these publications are related to the statics or dynamics of plates in the low-frequency band. The publications about high-frequency band, especially for dynamic problems, are limited.

For a long time, it seemed virtually impossible to incorporate short-wave high-frequency motion into low-dimensional structural models using a mathematically rational reasoning. The main point was that typical longitudinal wavelength is of the order of thickness for short-wave high-frequency motions. Thus, PDEs governing this type of motion should necessarily contain the derivatives both along the mid-plane and thickness. As a result, the dimension reduction was hardly possible. A new possibility for constructing hyperbolic lower-dimensional models arises from the recently developed explicit asymptotic models for surface waves on an elastic half-plane (see, [19]). In the framework of these models a 1D hyperbolic equation on the surface may be extracted. For a linear elastic isotropic half-plane $(-\infty < x_1 < \infty, 0 \leq x_3)$ under the transverse load P, this equation has the form

$$\frac{\partial^2 \Phi_s}{\partial x_1^2} - \frac{1}{c_{_R}^2} \frac{\partial^2 \Phi_s}{\partial t^2} = CP, \tag{1.1}$$

where $\Phi_s = \Phi(x_1, 0, t)$ is the value of the Lamé dilatation potential Φ on the surface, $c_{_R}$ the Raylegh velocity and C the function of material parameters. The boundary condition for the shear potential Ψ is given by

$$\frac{\partial \Psi}{\partial x_1} = -\frac{c_2^2}{2c_2^2 - c_{_R}^2} \frac{\partial \Phi}{\partial x_3} \qquad \text{at } x_3 = 0 \tag{1.2}$$

whereas the interior field is governed by the elliptic equations

$$\frac{\partial^2 \Phi}{\partial x_3^2} + \left(1 - \frac{c_{_R}^2}{c_1^2}\right) \frac{\partial^2 \Phi}{\partial x_1^2} = 0, \quad \frac{\partial^2 \Psi}{\partial x_3^2} + \left(1 - \frac{c_{_R}^2}{c_2^2}\right) \frac{\partial^2 \Phi}{\partial x_1^2} = 0 \tag{1.3}$$

with c_1 and c_2 being the dilatation and distortion wave velocities, respectively.

In this thesis, we attempt to derive a composite plate model incorporating

both long–wave low–frequency and short-wave high-frequency limits corresponding to flexural and surface waves, respectively. To this end, we adapt for a plate in the limit ($l \ll h$) the technique developed for analysis surface waves on a half-space. For our problem Rayleigh-Lamb dispersion relations will be obtained with the aid of the composite method and the asymptotic behaviour of the plate for the first antisymmetric bending mode will be found by transandantal first order roots of the Rayleigh-Lamb dispersion equation. The bending behaviour of the plate will be investigated in the near zone (near load) and in the far zone (at infinity). The obtained results will be compared to a reliable exact solution to show the validity of the model. This asymptotic method is based on the asymptotic integration of partial differential equations developed by Goldenveizer [20]. Together with an asymptotic approach introduced by Kaplunov and Kossovich [21]. This method also provided alternative solutions to the 2D problems in literature by using the relations between the potentials given on the surface introduced by Chadwick [22]. The sensitivity of the results obtained in the works [23], [24] and [25] indicates that it is quite possible to achieve similar results for the problems proposed in this thesis.

The organisation of the thesis is described as follows. After the Introduction given in Section 1, basic mathematical preliminaries and some definitions are given by Section 2.

Section 3 starts with the statement of the antisymmetric deformation of an elastic plate subjected to normal stress, antisymmetric plate modes are used for this problem. The composite equation for described elastic body is established with the help of asymptotic expansions given by [26] in terms of vertical displacement u_3. Then dispersion analysis done for both long–wave low–frequency and short–wave high–frequency limits, also displacement amplitudes are obtained. In Section, the composite equation for horizontal displacement is established with a similar approach with . Dispersion and displacement amplitudes are discussed as well. Section concludes with the illustrations of numerical results of the obtained asymptotic formulae and presents the accuracy of the asytpmtotic equations by comparison with the exact solutions. In Appendix the exact solutions for both horizontal and vertical displacement components.

In Section 4, our concern is the extension of an infinite elastic strip and es-

tablish a composite model for horizontal displacement component with symmetric modes. We follow similar asymptotic process as we did previous problems, and dispersion analysis done for this case, too. Composite equation and exact solution compared with the help of numerical results.

Finally, In Chapter 5, conclusions are given and the main results of the thesis are discussed.

2. MATHEMATICAL PRELIMINARIES

In this section we only mention some basic concepts and definitions of the theory of elasticity that will be used in the sequel.

2.1. State of stress

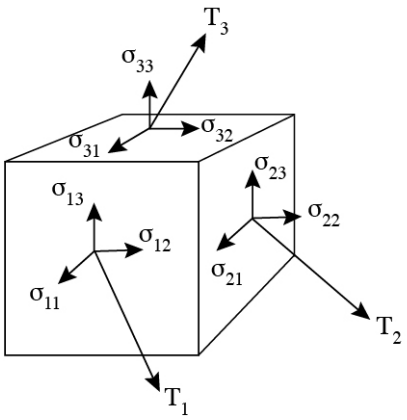

Figure 2.1. Components of stress

Let us consider a body oriented by the unit normal $\mathbf{n}$ with a number of acting on it. Taking an element with an area ΔA_n on the body and let the total force ΔF_n acts on this small area. Then the stress vector is defined as

$$\lim_{\Delta A_n -> 0} \frac{\Delta \mathbf{F}_n}{\Delta A_n} = \frac{d\mathbf{F}_n}{dA_n} = \mathbf{T}_n. \tag{2.1}$$

In general, the stress vector can have any direction to the surface area ΔA_n. $\mathbf{T}_n$ may be regarded as the sum of normal and tangential components. It is possible to find components of stress vector acting on a particular object by taking an infinitesimal cubic element, see Figure (2.1). The traction $\mathbf{T}_i$ acts on each face in following form

$$\mathbf{T}_i = \sigma_{ij} e_j, \quad i, j = 1, 2, 3, \tag{2.2}$$

where e_i is unit vector and a summation is assumed a repeating indices. Here σ_{ij} is coefficient of Cauchy stress tensor which is defined as

$$\sigma = \begin{bmatrix} \sigma_{11} & \sigma_{12} & \sigma_{13} \\ \sigma_{21} & \sigma_{22} & \sigma_{23} \\ \sigma_{31} & \sigma_{32} & \sigma_{33} \end{bmatrix} \tag{2.3}$$

If the traction $\mathbf{T}_n = (T_i)$ acts on an arbitrary surface oriented by unit normal $\mathbf{n} = (n_i)$ then the traction components can be written as

$$T_i = \sigma_{ji} n_j. \tag{2.4}$$

2.2. State of strain

Definition 2.1. *The relative change in the position of points in the body that has undergone deformation due to external or internal forces is called strain and shown as ϵ. The strain, ϵ, of a material linee element is expressed as the change in the length Δl per unit of the original length l of the line element;*

$$\epsilon = \frac{\Delta l}{l}. \tag{2.5}$$

The strain is positive if the object is stretched and negative if the object is compressed. As can be seen from the definition of the strain, unlike stress, strain is a dimensionless expression.

Strain may also be classified as normal and shear strains. Normal strain measures changes in length along a specific direction due to an applied force. It is also called extensional strain or dimensional strain and shown as ϵ_{ii}. So ϵ_{11} is the relative elongation or contraction of the length of the material along the x_1 axis. Shear strain measures changes in angle with respect to two specific directions. It is shown as ϵ_{ij} $(i \neq j)$. As an example, ϵ_{12} gives the angular change between the x_1 and x_2 axes. The normal and the shear strains, in literature, are sometimes shown as σ_{ii} and γ_{ij} $(i \neq j)$ respectively. However we will use σ_{ii} and σ_{ij} $(i \neq j)$ for the normal and shear stress respectively.

Let the component of a vector field **u(x)** be denoted by $u_i(x_1, x_2, x_3)$. If the functions $u_i(x_1, \ldots, x_n)$ are differentiable then the partial derivatives of the displacement may be denoted by the indicial notation as $u_{i,j} = \partial u_i / \partial x_j$. Hence the infinitesimal strain-displacement relationships can be given with the indicial notation as

$$\epsilon_{ij} = \frac{1}{2}(u_{i,j} + u_{j,i}). \tag{2.6}$$

2.3. Stress-strain relations

The most famous and elementary relation of the material behaviour is Hooke's law which states that deformation of the elastic material is proportional to applied force. This can be expressed mathematically as

$$F = kx, \tag{2.7}$$

where F is the force applied to the material and x is the displacement. Since stress is a force and strain is a displacement, the stresses and strains of the materials are connected by a *linearized* relationship that is mathematically similar to Hooke's law, and is often referred to by the same name. Therefore in one dimension, the relation between the stress and strain can be presented as

$$\sigma_{11} = E\epsilon_{11}, \tag{2.8}$$

where E is called modulus of elasticity or Young's modulus. In general, Hooke's law, relating the stress tensor to the strain, is written in the form of a fourth-order tensor as

$$\sigma_{ij} = E_{ijkl}\epsilon_{kl}, \tag{2.9}$$

where the 81 coefficients E_{ijkl} are called elastic constants. Taking into account certain material and geometric properties (symmetry, etc) of the elastic medium as well as symmetry of the stress tensor, the number of elastic constants reduce to 21. A material exhibiting different properties in different directions is called anisotropic. In the anisotropic materials these coefficients cannot be reduced any further. Therefore it will be first assumed that the material is independent from any

directions. In this case number of the elastic constants is reduced to 9 producing an orthotropic material which has 3 mutually orthogonal planes of elastic symmetry. Finally for an additional simplification, directional and rotational independence is assumed. This assumption reduces the number of the constants to 2 producing an isotropic material which has uniform physical properties in all orientations. Thus the relation between the stress and strain can be written as

$$\sigma_{ij} = \lambda \epsilon_{kk} \delta_{ij} + 2\mu \epsilon_{ij}, \tag{2.10}$$

where λ and μ are known as Lamé constants and δ_{ij} is Kronecker delta. If the strain-displacement relations given by equation (2.5) are substituted into the above equality, stress-displacement relations is written as

$$\sigma_{ij} = \lambda u_{k,k} \delta_{ij} + \mu (u_{i,j} + u_{j,i}), \tag{2.11}$$

see If these relations are written in an explicit form, we have for $i = 1, 2$, $j = 1, 2$ $(i \neq j)$, and $k = 1, 2, 3$

$$\begin{aligned} &\sigma_{ij} = \mu\left(\frac{\delta u_i}{\delta x_j} + \frac{\delta u_i}{\delta x_j}\right), \quad \sigma_{ii} = (\lambda + 2\mu)\frac{\delta u_i}{\delta x_i} + \lambda\left(\frac{\delta u_j}{\delta x_j} + \frac{\delta u_3}{\delta x_3}\right), \\ &\sigma_{3i} = \sigma_{i3} = \mu\left(\frac{\delta u_i}{\delta x_3} + \frac{\delta u_3}{\delta x_i}\right), \quad \sigma_{33} = \lambda\left(\frac{\delta u_i}{\delta x_i} + \frac{\delta u_j}{\delta x_j}\right) + (\lambda + 2\mu)\frac{\delta u_3}{\delta x_3}. \end{aligned} \tag{2.12}$$

It is also known from Hooke's law that the relation between the stress and strain in one dimension can be expressed by equation (2.8). Therefore if equation (2.8) is substituted into equation (2.10), the following equality is obtained.

$$\sigma_{11} = \frac{\mu(3\lambda + 2\mu)}{\mu + \lambda} \epsilon_{ij}. \tag{2.13}$$

This equality gives us Young's modulus, E, in terms of the Lamé constants as

$$E = \frac{\mu(3\lambda + 2\mu)}{\mu + \lambda}. \tag{2.14}$$

Another important elastic coefficient different from aforementioned coefficient is

Poisson's ratio ν. Poisson's ratio is the negative ratio of transverse strain to the axial strain in the direction of the applied load. When a load is applied to a material, the material tends to expand or contract in the other two directions perpendicular to the direction of the load. This transverse change will bear a fixed relationship to the axial strain. The relationship, or ratio, of the transverse strain is called Poisson's ratio. If the subscript 1 corresponds to the axial direction and subscripts 2 and 3 correspond to the transverse directions then Poisson's ratio can be written as

$$\nu = -\frac{\epsilon_{22}}{\epsilon_{11}} = -\frac{\epsilon_{33}}{\epsilon_{11}} = \frac{\lambda}{2(\mu + \lambda)}. \tag{2.15}$$

Since λ must remain finite, Poisson's ratio lies between $-1 < \nu < 0.5$.

2.4. Governing equations of the theory of elastic plates

In this section, we present the fundamental equations of the theory of thin plates. Let us consider a thin elastic plate of infinite length along the directions x_1 and x_2 with thickness $2h$, where x_1, x_2 and x_3 denote Cartesian coordinates $(-\infty < x_1, x_2 < \infty, \quad -h < x_3 < +h)$. In the classical elastic thin plate theory, there are certain assumptions that are necessary in order to derive the equations of motion. For a thin plate described above, the following assumptions are made, see [28],

1. A lineal element of the plate extending through the plate thickness, normal to the midsurface, $x_1 - x_2$ plane, in the unstressed state, upon the application of load:

   a. undergoes at most a translation and a rotation with respect to the original coordinate system,

   b. remains normal to the deformed middle surface.

2. A plate resists lateral and in-plane loads by bending, transverse shear stresses, and in-plane action, not through block like compression or tension in the plate in the thickness direction. This assumption results from the fact that $\eta = h/R$ (R is a typical radius of curvature of the midsurface).

3. A lineal element through the thickness does not elongate or contract.

4. The lineal element remains straight upon load application.

Apart from the small parameter η, thin elastic plates are also characterized by L, a typical wavelength and T, the time scale. The equation of motion is given by

$$\frac{E}{2(1+\nu)}\Delta\mathbf{u} + \frac{E}{2(1+\nu)(1-2\nu)}\text{grad div}\mathbf{u} - \rho\frac{\partial^2\mathbf{u}}{\partial t^2} = 0 \tag{2.16}$$

where $\mathbf{u} = (u_1, u_2, u_3)$ is displacement vector, Δ is Laplacian operator, E is Young's modulus, ν is Poisson's ratio, ρ is density and t is time.

Poisson's ratio, also called the Poisson coefficient, is the ratio of transverse contraction strain to longitudinal extension strain in stretched bar. Traditionally the Poisson's ratio was always assumed positive, $0 < \nu < .5$*, since everyday materials get thinner when stretched. Today it has been shown through numerous studies that materials with negative Poisson's ratio also exist, extending the range to* $-1 < \nu < 0.5$.

We always assume that the geometrical parameter $\eta = h/R$ (R is a typical radius of curvature of the midsurface) is small, i.e. in this thesis we consider only thin walled bodies. Apart from the geometrical parameter η, dynamic processes in thin walled bodies are characterised by two physical parameters l, the ratio of the wavelength to R and T the ratio of the time scale to Rc_2^{-1}, where c_2 is the shear wave speed. It is convenient to express these two parameters in terms of the small parameter η

$$l = n^q \quad \text{and} \quad T = \eta^a,$$

where q and a are called the variability and dynamicity indices, respectively. Let us introduce the classification of the asymptotic approximations under consideration, see Figure (2.2)

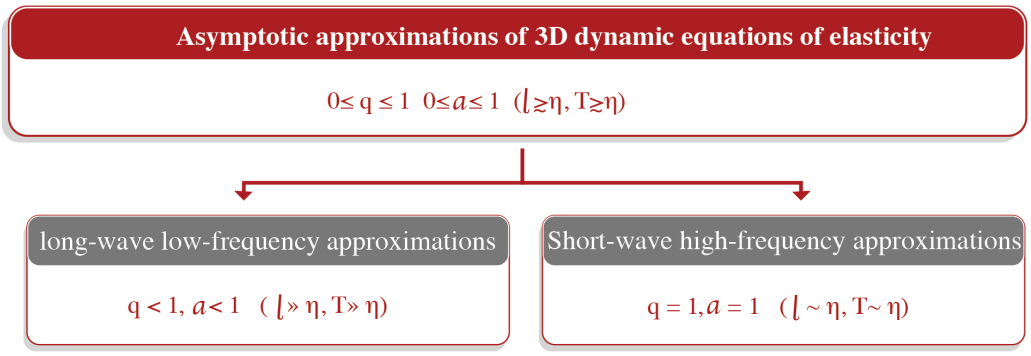

Figure 2.2. Asymptotic approximations of 3D dynamic equations of elasticity

In order to write the equations of motion of plane elasticity we refer to equations (1.1.1)-(1.1.5) in [26] and reduce them, in the setup above, to the following equations:

$$\begin{aligned}
\sigma_{11} &= \frac{E}{2(1+\nu)\chi^2}\left(\frac{\partial u_1}{\partial x_1} + \frac{\nu}{1-\nu}\frac{\partial u_3}{\partial x_3}\right),\\
\sigma_{22} &= \frac{E\nu}{2(1-\nu^2)\chi^2}\left(\frac{\partial u_1}{\partial x_1} + \frac{\partial u_3}{\partial x_3}\right),\\
\sigma_{33} &= \frac{E\nu}{2(1+\nu)\chi^2}\left(\frac{\nu}{1-\nu}\frac{\partial u_1}{\partial x_1} + \frac{\partial u_3}{\partial x_3}\right),\\
\sigma_{31} &= \frac{E\nu}{2(1+\nu)}\left(\frac{\partial u_3}{\partial x_1} + \frac{\partial u_1}{\partial x_3}\right),
\end{aligned} \tag{2.17}$$

where

$$\chi = \frac{c_2}{c_1} = \sqrt{\frac{1-2\nu}{2(1-\nu)}} \tag{2.18}$$

where c_1 and c_2 are respectively the longitudinal and shear wave speeds given by

$$c_1 = \sqrt{\frac{E(1-\nu)}{(1+\nu)(1-2\nu)\rho}}, \qquad c_2 = \sqrt{\frac{E}{2(1+\nu)\rho}}. \tag{2.19}$$

According to the Helmholtz decomposition theorem, any vector field can be represented by a combination of the gradient of a scalar potential and the curl of a

vector potential, see [30], that is

$$\mathbf{u} = \text{grad}\phi + \text{curl}\mathbf{\Psi}, \tag{2.20}$$

where ϕ is a scalar potential, $\mathbf{\Psi} = (\psi_1, \psi_2, \psi_3)$ is a vector potential and $\mathbf{u} = (u_1, u_2, u_3)$ is the displacement vector. On employing equation (2.20) the components of $\mathbf{u}$, in terms of wave potentials, are given by

$$u_1 = \frac{\partial \phi}{\partial x_1} + \frac{\partial \psi_3}{\partial x_2} - \frac{\partial \psi_2}{\partial x_3}, \tag{2.21}$$

$$u_2 = \frac{\partial \phi}{\partial x_2} - \frac{\partial \psi_3}{\partial x_1} + \frac{\partial \psi_1}{\partial x_3}, \tag{2.22}$$

and

$$u_3 = \frac{\partial \phi}{\partial x_3} + \frac{\partial \psi_2}{\partial x_1} - \frac{\partial \psi_1}{\partial x_2}. \tag{2.23}$$

Throughout the thesis, we shall only consider propagation in the $x_1 - x_3$ plane, so setting $\dfrac{\partial}{\partial x_2} = 0$ in (2.21), (2.22) and (2.23) gives us

$$u_1 = \frac{\partial \phi}{\partial x_1} - \frac{\partial \psi_2}{\partial x_3}, \tag{2.24}$$

$$u_2 = -\frac{\partial \psi_3}{\partial x_1} + \frac{\partial \psi_1}{\partial x_3}, \tag{2.25}$$

and

$$u_3 = \frac{\partial \phi}{\partial x_3} + \frac{\partial \psi_2}{\partial x_1}. \tag{2.26}$$

Substituting (2.24) and (2.26) into (2.16) we obtain a pair of wave equations in the potentials ϕ and ψ given by

$$\Delta\phi - \frac{1}{c_1^2}\frac{\partial^2 \phi}{\partial t^2} = 0, \qquad \Delta\psi - \frac{1}{c_2^2}\frac{\partial^2 \psi}{\partial t^2} = 0. \tag{2.27}$$

with the assumption $\Psi = (0, 0, -\psi)$. The derivation of the asymptotic equations requires an appropriate scaling of the spatial and time variables. We choose scalings of the variables as x_1 and x_3 balanced with the half-thickness h and, the time variable

t with the ratio of h and shear wave c_2. We thus introduce

$$x_1 = \xi h, \quad x_3 = \zeta h \quad \text{and} \quad t = \frac{\tau h}{c_2}. \tag{2.28}$$

where ξ and ζ are dimensionless longitudinal and vertical coordinates, and τ is the dimensionless time variable. We may also scale the wavenumber k and angular frequency ω as

$$K = kh \qquad \Omega = \frac{\omega h}{c_2}. \tag{2.29}$$

Here K and Ω are dimensionless wavenumber and angular frequency, respectively. Let us now seek the plane travelling wave solution to equations (2.27) in the form

$$\begin{aligned} \psi &= f(\zeta) e^{i(K\xi - \Omega\tau)} \\ \phi &= g(\zeta) e^{i(K\xi - \Omega\tau)} \end{aligned} \tag{2.30}$$

where $i = \sqrt{-1}$. Inserting (2.30) into equations (2.27) we obtain the following hyperbolic equations

$$\begin{aligned} \frac{\partial^2 f}{\partial \zeta^2} - \alpha^2 f = 0, \\ \frac{\partial^2 g}{\partial \zeta^2} - \beta^2 g = 0 \end{aligned} \tag{2.31}$$

where

$$\alpha = \sqrt{K^2 - \chi^2 \Omega^2}, \qquad \beta = \sqrt{K^2 - \Omega^2}. \tag{2.32}$$

There are two groups of vibration modes corresponding the equations given by (2.31), namely antisymmetric and symmetric modes with respect to the midsurface. These modes will be described in detail in the following sections.

2.5. Antisymmetric modes of an elastic plate

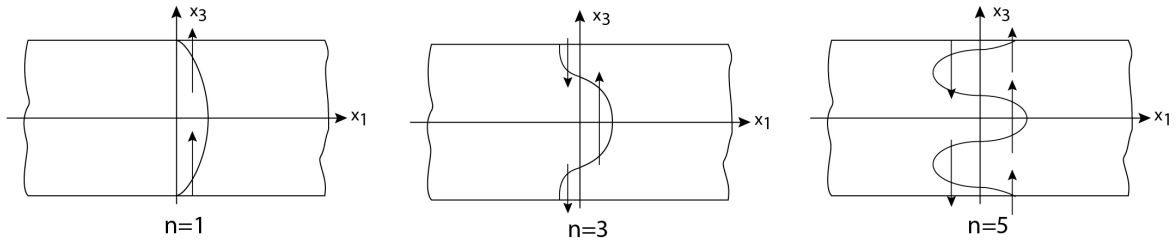

Figure 2.3. First three antisymmetric modes of vertical displacement component

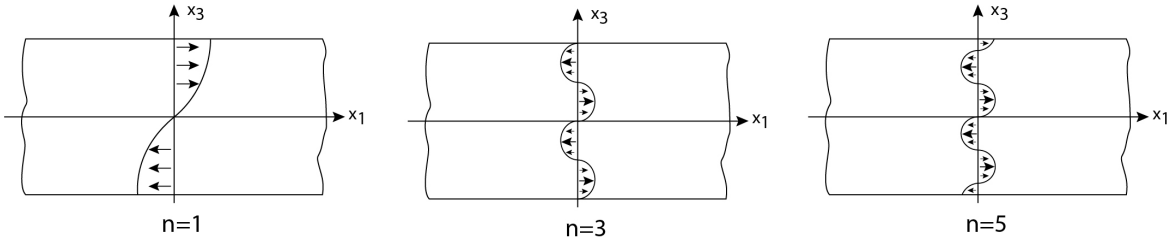

Figure 2.4. First three antisymmetric modes of horizontal displacement component

In order to obtain the antisymmetric modes in case of plate bending we seek the solution of (2.31) in the form

$$f = A\sinh(\alpha\zeta), \qquad g = B\cosh(\beta\zeta). \tag{2.33}$$

In this case, the displacement u_1 and the stresses σ_{11}, σ_{22}, σ_{33} are odd with respect to ζ while displacement u_3 and the stress σ_{31} are even.

Let us first write down the 2D equations governing the long-wave low-frequency approximations, for which

$$L \gg h, \qquad T \gg \sqrt{\frac{\rho}{E}}h. \tag{2.34}$$

It is well known that this approximation corresponds to the classical Kirchhoff theory for plate bending resulting in the fourth-order parabolic equation

$$D\Delta^2 w + 2\rho h\frac{\partial^2 w}{\partial t^2} - Q_N - 2h\mathrm{div}_\Gamma \mathbf{Q}_T = 0, \tag{2.35}$$

where w is the vertical displacement of the mid plane ($w = u_3|_{x_3=0}$), Q_N is vertical

load, $\mathbf{Q}_T = (Q_1, Q_2)$ is the vector of tangential loads, the bending stiffness D is given by

$$D = \frac{2Eh^3}{3(1-\nu^2)}, \tag{2.36}$$

and the 2D operator div_Γ is given by

$$\mathrm{div}_\Gamma \mathbf{Q}_T = \frac{\partial Q_1}{\partial x_1} + \frac{\partial Q_2}{\partial x_2}. \tag{2.37}$$

2.6. Symmetric modes of an elastic plate

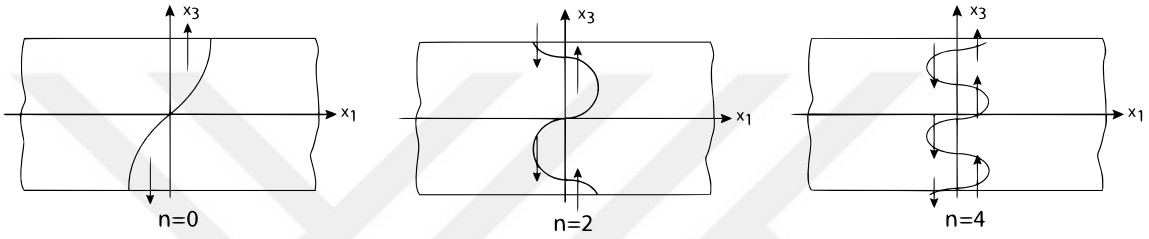

Figure 2.5. First three symmetric modes of vertical displacement component

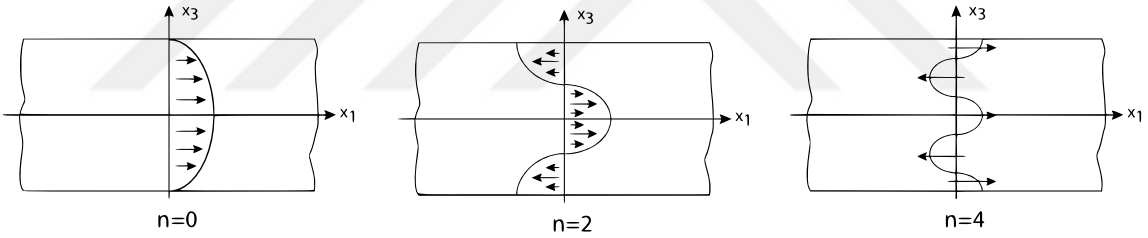

Figure 2.6. First three symmetric modes of horizontal displacement component

Similar to the previous case, assuming (2.31)

$$f = A\cosh(\alpha\zeta), \qquad \beta = B\sinh(\beta\zeta) \tag{2.38}$$

gives us symmetric modes for plate extension and transverse compression of a thin plate. For symmetric modes the displacement u_1 and the stresses σ_{11}, σ_{22}, σ_{33} are even with respect to ζ while displacement u_3 and the stress σ_{31} are odd.

For this case the governing equation is given by

$$Eh\left(\frac{1}{1+\nu}\Delta\mathbf{u} + \frac{1}{1-\nu}\mathrm{graddiv}\mathbf{u}\right) - 2\rho h\frac{\partial^2\mathbf{u}}{\partial t^2} + 2\mathbf{Q}_T + \frac{2h\nu}{1-\nu}\mathrm{grad}Q_3 = 0. \tag{2.39}$$

Similarly, we may also write the refined equation by adding $O(\eta^2)$ and $O(\eta^4)$ terms

into (2.39)

$$
\begin{aligned}
&Eh\left(\frac{1}{1+\nu}\Delta\mathbf{u}+\frac{1}{1-\nu}\text{grad div}\mathbf{u}\right)-2\rho h\frac{\partial^2\mathbf{u}}{\partial t^2}+2\mathbf{Q}_T+\frac{2h\nu}{1-\nu}\text{grad}Q_3+\\
&Eh^3\left[-\frac{1}{6(1+\nu)}\Delta^2\mathbf{u}-\frac{3+4\nu-\nu^2}{6(1-\nu)^2(1+\nu)}\Delta\text{grad div}\mathbf{u}+\frac{2\rho}{3E}\frac{\partial^2}{\partial t^2}\Delta\mathbf{u}\right.\\
&-\frac{2(1+\nu)\rho^2}{3E^2}\frac{\partial^4\mathbf{u}}{\partial t^4}+\frac{(2+\nu-\nu^2)\rho}{3(1-\nu)^2E}\frac{\partial^2}{\partial t^2}\text{grad div}\mathbf{u}-\frac{1+2\nu^2}{3(1-\nu)^2E}\Delta\text{grad}Q_3\\
&\left.+\frac{(1+\nu)(1-3\nu+4\nu^2)\rho}{3(1-\nu)^2E^2}\frac{\partial^2}{\partial t^2}\text{grad}Q_3\right]=0.
\end{aligned}
\tag{2.40}
$$

2.7. Asymptotic model for Surface Waves

Since we are trying to establish a composite equation, we need to compare the equation that we aim to obtain when $L \gg h$, with the plate limit . When $L \ll h$, the plate behaves like a half-space and the waves generated in this case will behave like surface waves, see Fig 2.7. That's why we're trying to obtain an asymptotic model for Rayleig Surface Waves.

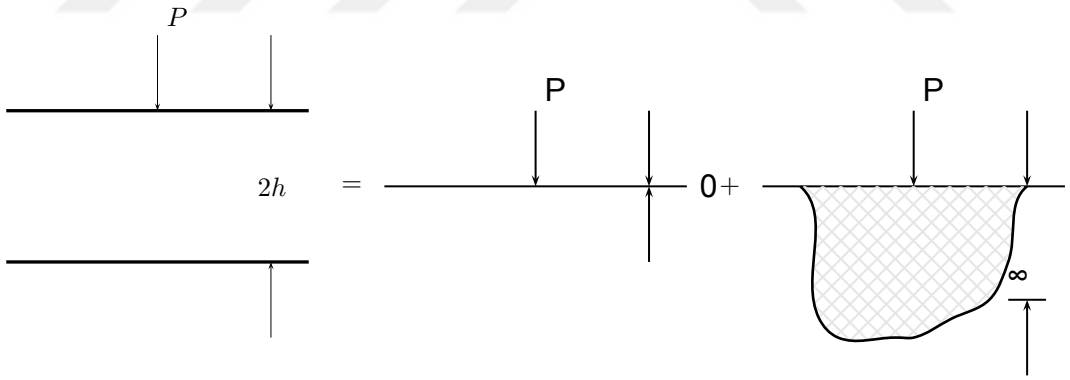

Figure 2.7. Behaviour of plate waves

To this end, we follow the exposition given in [30]. Let us give the asymptotic formulation for Rayleigh wave, which is valid at

$$L \ll h \quad \text{and} \quad T \ll \sqrt{\frac{\rho}{E}}h. \tag{2.41}$$

At leading order, this is given by a 2D hyperbolic equation along each of the faces $x_3 = \pm h$, due to the symmetry, below we consider only the upper face $x_3 = h$. In

terms of the boundary value of the scalar wave potential $\phi(x_1, x_2, x_3, t)$ we have

$$\Delta\phi_h - \frac{1}{c_R^2}\frac{\partial^2\phi_h}{\partial t^2} = -\frac{1+k_2^2}{4\mu B}P, \tag{2.42}$$

where $\phi_h = \phi(x_1, x_2, h, t)$, μ is Lamé elastic modulus, c_R is the Rayleigh wave speed, P is the normal load corresponding to Q_N defined above, and

$$B = \frac{k_1}{k_2}(1-k_1^2) + \frac{k_2}{k_1}(1-k_2^2) - (1-k_2^4), \tag{2.43}$$

with

$$k_i = \sqrt{1 - \frac{c_R^2}{c_i^2}}, \qquad i = 1, 2. \tag{2.44}$$

Over the interior $|x_3| < h$, $\phi(x_1, x_2, x_3, t)$ satisfies the elliptic equation

$$\frac{\partial^2\phi}{\partial x_3^2} + k_1^2\Delta\phi = 0, \tag{2.45}$$

whereas a pair of shear potentials $\Psi_i(x_1, x_2, x_3, t)$, $i = 1, 2$, may be found from the boundary value problem

$$\frac{\partial^2\Psi_i}{\partial x_3^2} + k_2^2\Delta\Psi_i = 0, \tag{2.46}$$

with

$$\left.\frac{\partial\Psi_i}{\partial x_3}\right|_{x_3=h} = \frac{1+k_2^2}{2}\frac{\partial\Phi_h}{\partial x_i}. \tag{2.47}$$

Hyperbolic equation (2.42) may also be written through the displacements of the upper face $u_i(x_1, x_2, x_3, t)$, $i = 1, 2, 3$. To this end, we express the solutions of elliptic equations (2.45) and (2.46) as

$$\Phi = \Phi_h e^{\sqrt{-\Delta}k_1(x_3-h)} \quad \text{and} \quad \Psi_i = \Psi_{ih} e^{\sqrt{-\Delta}k_2(x_3-h)}, \tag{2.48}$$

where $\sqrt{-\Delta}$ is a 2D pseudo-differential operator and $\Psi_{ih} = \Psi_i(x_1, x_2, h, t)$. Then, taking into account the boundary condition (2.47) and also the relation

$$\left.\frac{\partial\Phi_h}{\partial x_3}\right|_{x_3=h} = -\frac{1+k_2^2}{2}\left(\frac{\partial\Psi_{1h}}{\partial x_1} + \frac{\partial\Psi_{2h}}{\partial x_2}\right), \tag{2.49}$$

we obtain

$$u_i = \frac{\partial \Psi_i}{\partial x_3} - \frac{\partial \Phi_h}{\partial x_i}\bigg|_{x_3=h} = -\frac{1-k_2^2}{2}\frac{\partial \Phi_h}{\partial x_i}, \qquad i = 1, 2, \tag{2.50}$$

and

$$u_3 = \frac{\partial \Phi}{\partial x_3}\bigg|_{x_3=h} + \frac{\partial \Psi_{1h}}{\partial x_1} + \frac{\partial \Psi_{2h}}{\partial x_2} = \frac{k_1(1-k_2^2)}{1+k_2^2}\sqrt{-\Delta}\,\Phi_h. \tag{2.51}$$

With the help of these formulae, we may write the equation (2.42), which is written in terms of potential Φ_h, in terms of displacement components as

$$\Delta u_i - \frac{1}{{c_R}^2}\frac{\partial^2 u_i}{\partial t^2} = -\frac{(1-k_2^4)}{8\mu B}\frac{\partial P}{\partial x_i}, \quad i = 1, 2 \tag{2.52}$$

or

$$\Delta u_3 - \frac{1}{c_R^2}\frac{\partial^2 u_3}{\partial t^2} = -\frac{k_1(1-k_2^2)}{4\mu B}\sqrt{-\Delta}P. \tag{2.53}$$

Thus, we have obtained the Rayleigh equation, that is given in terms of scalar wave potential Φ_h, in terms of displacement components.

3. COMPOSITE WAVE MODELS FOR ELASTIC PLATE

In this section, we attempt to establish 2D composite hyperbolic equations for an elastic plate using Kirchhoff or refined asymptotic plate equations along with the Rayleigh wave equation, regarding the idea of composite equations incorporating both long and short-wave limiting forms, for which a typical wavelength is much greater or smaller than the plate thickness. We restrict ourselves to surface loading, when bending and Rayleigh waves are seemingly of the most importance. We do not expect, from the very beginning, to arrive at uniformly valid composite equations. The point is that over the intermediate range, for which a wavelength is of order of thickness, a plate demonstrates essentially 3D behaviour, which does not allow any asymptotic dimension reduction.

3.1. Statement of the Problem

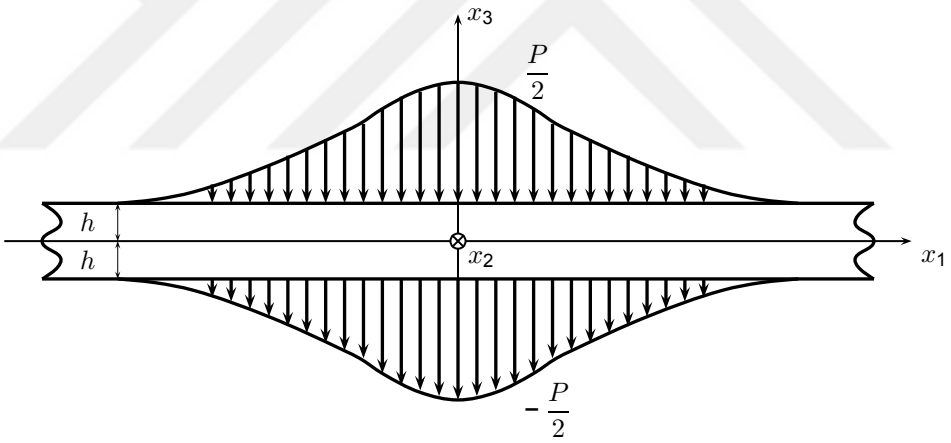

Figure 3.1. Antisymmetric deformation of an elastic layer under normal surface loading

We consider antisymmetric deformation of an elastic plate subjected to prescribed normal stress $\pm\frac{1}{2}P(x_1, x_2, t)$ at the faces $x_3 = \pm h$, respectively, as given in Figure 3.1. For long-wave low-frequency approximation the governing equation can be written by taking $Q_T = 0$ in the Kirchoff plate equation (2.35)

$$D\Delta^2 w + 2\rho h\frac{\partial^2 w}{\partial t^2} = P, \tag{3.1}$$

where we adopt the notation $Q_N = P$. In this case we have no tangential loading but normal loading, so we may obtain the refined plate equation for this problem

by taking $Q_T = 0$ and $Q_N = P$ in (3.20)

$$D\Delta^2 w + 2\rho h \left(1 + h^2 \frac{7\nu - 17}{15(1-\nu)}\Delta\right) \frac{\partial^2 w}{\partial t^2} = \left(1 - h^2 \frac{8 - 3\nu}{10(1-\nu)}\Delta\right) P. \tag{3.2}$$

To obtain the relation between w and the displacement components u_1, u_2, we may use the following results from analysis of higher order plate bending theory in Chapter7 in [26]

$$\begin{aligned} u_3 &= R u_3^* \\ u_i &= R v_i^* \\ Q_3^* &= \frac{1}{E}\eta Q_3. \end{aligned} \tag{3.3}$$

where η and R are given in Section 2.4, and the starred quantities are of the same asymptotic order, and independent of the thickness variable ζ.

$$\begin{aligned} u_3^* &= w + \eta^2 \zeta^2 u_3^{(2)}, \\ u_i^* &= \zeta u_i^{(1)} + \eta^2 \zeta^3 u_i^{(3)} \quad i = 1, 2. \end{aligned} \tag{3.4}$$

Employing a two–term asymptotic expansion in ζ, it is possible to obtain asymptotic expansions for displacements and stresses given by

$$
\begin{aligned}
u_i^{(1)} &= -\frac{\partial w}{\partial \xi_i} + \eta^2 2(1+\nu)\sigma_{3i}^{(0)}, \\
\sigma_{ii}^{(1)} &= \frac{1}{1-\nu^2}\left(\frac{\partial u_i^{(1)}}{\partial \xi_i} + \nu \frac{\partial u_j^{(1)}}{\partial \xi_j}\right) + \eta^2 \frac{\nu}{1-\nu}\sigma_{33}^{(1)}, \\
\sigma_{ij}^{(1)} &= \frac{1}{2(1+\nu)}\left(\frac{\partial u_i^{(1)}}{\partial \xi_j} + \frac{\partial u_j^{(1)}}{\partial \xi_i}\right), \\
\sigma_{3i}^{(2)} &= -\frac{1}{2}\left(\frac{\partial \sigma_{ii}^{(11)}}{\partial \xi_i} + \frac{\partial \sigma_{ij}^{(1)}}{\partial \xi_j}\right) + \eta^2 \frac{1}{4(1+\nu)}\frac{\partial^2 u_i^{(1)}}{\partial \tau^2}, \\
\sigma_{3i}^{(0)} &= -\sigma_{3i}^{(2)} - \eta^2 \sigma_{3i}^{(4)}, \\
\sigma_{33}^{(1)} &= -\frac{\partial \sigma_{3i}^{(0)}}{\partial \xi_i} - \frac{\partial \sigma_{3j}^{(0)}}{\partial \xi_j} + \frac{1}{2(1+\nu)}\frac{\partial^2 w}{\tau^2}, \\
\sigma_{33}^{(3)} &= -\frac{1}{3}\left(\frac{\partial \sigma_{3i}^{(2)}}{\partial \xi_i} + \frac{\partial \sigma_{3j}^{(2)}}{\partial \xi_j}\right) + \eta^2 \frac{1}{6(1+\nu)}\frac{\partial^2 u_3^{(2)}}{\partial \tau^2} \quad (i \neq j = 1, 2).
\end{aligned}
\tag{3.5}
$$

Constitutive equations as well as boundary conditions are given in the following form

$$
\begin{aligned}
u_3^{(2)} &= -\frac{1}{2}\nu\left(\sigma_{ii}^{(1)} + \sigma_{jj}^{(1)}\right), \\
u_i^{(3)} &= -\frac{1}{3}\frac{\partial u_3^{(2)}}{\partial \xi_i} + \frac{2}{3}(1+\nu)\sigma_{3i}^{(2)}, \\
\sigma_{ii}^{(3)} &= \frac{1}{1-\nu^2}\left(\frac{\partial u_i^{(3)}}{\partial \xi_i} + \nu \frac{\partial u_j^{(3)}}{\partial \xi_j}\right) + \frac{\nu}{1-\nu}\sigma_{33}^{(3)}, \\
\sigma_{ij}^{(3)} &= \frac{1}{2(1+\nu)}\left(\frac{\partial u_i^{(3)}}{\partial \xi_j} + \frac{\partial u_j^{(3)}}{\partial \xi_i}\right), \\
\sigma_{3i}^{(4)} &= -\frac{1}{4}\left(\frac{\partial \sigma_{ii}^{(3)}}{\partial \xi_i} + \frac{\partial \sigma_{ij}^{(3)}}{\partial \xi_j}\right), \\
\sigma_{33}^{(5)} &= -\frac{1}{5}\left(\frac{\partial \sigma_{3i}^{(4)}}{\partial \xi_i} + \frac{\partial \sigma_{3j}^{(4)}}{\partial \xi_j}\right).
\end{aligned}
\tag{3.6}
$$

On the surface $\zeta = 1$ from (3.4), we have

$$
u_3^* = w + \eta^2 u_3^{(2)} \tag{3.7}
$$

and employing the relevant identities of (3.4)–(3.6) in (3.7), we get

$$
\begin{aligned}
u_3^* &= w - \eta^2 \frac{\nu}{2}\left(\sigma_{ii}^{(1)} + \sigma_{jj}^{(1)}\right) + O(\eta^4), \qquad (3.8)\\
&= w - \eta^2 \frac{\nu}{2(1-\nu^2)}\left(\frac{\partial u_i^{(1)}}{\partial \xi_i} + \nu\frac{\partial u_j^{(1)}}{\partial \xi_j} + \frac{\partial u_j^{(1)}}{\partial \xi_j} + \nu\frac{\partial u_i^{(1)}}{\partial \xi_i}\right) + O(\eta^4),\\
&= w - \eta^2 \frac{\nu}{2(1-\nu)}\left(\frac{\partial u_i^{(1)}}{\partial \xi_i} + \frac{\partial u_j^{(1)}}{\partial \xi_j}\right) + O(\eta^4),\\
&= w + \eta^2 \frac{\nu}{2(1-\nu)}\left(\frac{\partial^2 w}{\partial \xi_i^2} + \frac{\partial^2 w}{\partial \xi_j^2}\right) + O(\eta^4).
\end{aligned}
$$

Since the problem is independent of the horizontal coordinate ξ_2, we may write $\dfrac{\partial}{\partial \xi_2} = 0$, and for ease of reference we set $\xi_1 = \xi$. Ignoring the higher order terms $O(\eta^4)$ in equation 3.8 we arrive at

$$u_3^* = \left(1 + \eta^2 \frac{\nu}{2(1-\nu)}\frac{\partial^2}{\partial \xi^2}\right) w \qquad (3.9)$$

Returning back to the original variables we may express the vertical displacement on the upper face $x_3 = h$, in terms of the mid plane displacement as

$$u_3 = \left(1 + h^2 \frac{\nu}{2(1-\nu)}\frac{\partial^2}{\partial x_1^2}\right) w. \qquad (3.10)$$

Thus, we have obtained the differential operator that gives the relationship between w and u_3

$$u_3 = L_3 w, \qquad (3.11)$$

with

$$L_3 = 1 + h^2 \frac{\nu}{2(1-\nu)}\frac{\partial^2}{\partial x_1^2}. \qquad (3.12)$$

For $u_i, i = 1, 2$, we have the following asymptotic relation

$$u_i^* = u_1^{(1)} + \eta^2 u_1^{(3)}. \qquad (3.13)$$

Following the same procedure as done for u_3, employing the relevant identities of

(3.4)–(3.6) and taking $i = 1$ in (3.4), we get

$$
\begin{aligned}
u_1^* &= u_i^{(1)} + \eta^2 u_i^{(3)} + O(\eta^4), \qquad (3.14)\\
&= -\frac{\partial w}{\partial \xi_i} + \eta^2 2(1+\nu)\sigma_{3i}^{(0)} - \eta^2 \frac{1}{3}\frac{\partial u_3^{(2)}}{\partial \xi} + \eta^2 \frac{2}{3}(1+\nu)\sigma_{3i}^{(2)} + O(\eta^4)\\
&= -\frac{\partial w}{\partial \xi_i} + \eta^2 \frac{\nu}{6}\left(\frac{\partial \sigma_{ii}^{(1)}}{\partial \xi_i} + \frac{\partial \sigma_{jj}^{(1)}}{\partial \xi_i}\right) + \eta^2 \frac{4(1+\nu)}{6}\left(\frac{\partial \sigma_{ii}^{(11)}}{\partial \xi_i} + \frac{\partial \sigma_{ij}^{(1)}}{\partial \xi_j}\right) + O(\eta^4)\\
&= -\frac{\partial w}{\partial \xi_i} + \eta^2 \frac{4+5\nu}{6}\frac{\partial \sigma_{ii}^{(1)}}{\partial \xi_i} + \eta^2 \frac{\nu}{6}\frac{\partial \sigma_{jj}^{(1)}}{\partial \xi_i} + \eta^2 \frac{4(1+\nu)}{6}\frac{\partial \sigma_{ij}^{(1)}}{\partial \xi_j} + O(\eta^4)\\
&= -\frac{\partial w}{\partial \xi_i} + \eta^2 \frac{4+5\nu}{6(1-\nu^2)}\left(\frac{\partial^2 u_i^{(1)}}{\partial \xi_i^2} + \nu\frac{\partial^2 u_j^{(1)}}{\partial \xi_i \partial \xi_j}\right) + \eta^2 \frac{\nu}{6(1-\nu^2)}\left(\frac{\partial^2 u_2^{(1)}}{\partial \xi_i \partial \xi_j} + \nu\frac{\partial^2 u_1^{(1)}}{\partial \xi_i^2}\right)\\
&\quad - \eta^2 \frac{2}{6}\left(\frac{\partial^2 u_i^{(1)}}{\partial \xi_i^2} + \frac{\partial^2 u_j^{(1)}}{\partial \xi_i \partial \xi_j}\right) + O(\eta^4)\\
&= -\frac{\partial w}{\partial \xi_i} + \eta^2 \frac{\nu+4}{6(1-\nu)}\frac{\partial^2 u_i^{(1)}}{\partial \xi_i^2} - \eta^2 \frac{3\nu+2}{6(1-\nu)}\frac{\partial^2 u_j^{(1)}}{\partial \xi_i \partial \xi_j} + \eta^2 \frac{2}{6}\frac{\partial^2 u_i^{(1)}}{\partial \xi_i^2} + O(\eta^4)\\
&= -\frac{\partial w}{\partial \xi_i} - \eta^2 \frac{\nu+4}{6(1-\nu)}\frac{\partial^3 w}{\partial \xi_i^3} + \eta^2 \frac{3\nu+2}{6(1-\nu)}\frac{\partial^3 w}{\partial \xi_i \partial^2 \xi_j^2} - \eta^2 \frac{2}{6}\frac{\partial^3 w}{\partial \xi_i \partial^2 \xi_j^2} + O(\eta^4),\\
&= -\frac{\partial w}{\partial \xi_i} - \eta^2 \frac{\nu+4}{6(1-\nu)}\frac{\partial^3 w}{\partial \xi_i^3} + \eta^2 \frac{5\nu}{6(1-\nu)}\frac{\partial^3 w}{\partial \xi_i \partial \xi_j^2} + O(\eta^4),\\
&= -\left(1 + \eta^2\left(\frac{\nu+4}{6(1-\nu)}\frac{\partial^2}{\partial \xi_i^2} + \frac{5\nu}{6(1-\nu)}\frac{\partial^2}{\partial \xi_j^2}\right)\right)\frac{\partial w}{\partial \xi_i} + O(\eta^4), \quad i \neq j = 1, 2.
\end{aligned}
$$

If we return back to the original variables in equation (3.14), we get

$$
u_i^* = -h\left(1 + h^2\left(\frac{\nu+4}{6(1-\nu)}\frac{\partial^2}{\partial x_i^2} - \frac{5\nu}{6(1-\nu)}\frac{\partial^2}{\partial x_j^2}\right)\right)\frac{\partial w}{\partial x_i}, \quad i \neq j = 1, 2. \qquad (3.15)
$$

Thus, we obtain the relation between u_i and w on the upper surface $x_3 = h$ given by

$$
u_i = L_i \frac{\partial w}{\partial x_i}, \qquad i = 1, 2, \qquad (3.16)
$$

with

$$
L_i = -h\left[1 + h^2\left(\frac{\nu+4}{6(1-\nu)}\frac{\partial^2}{\partial x_i^2} - \frac{5\nu}{6(1-\nu)}\frac{\partial^2}{\partial x_j^2}\right)\right], \quad i, j = 1, 2, \quad i \neq j, \qquad (3.17)
$$

Hence, with the help of asymptotic expansions of displacement components we found the differential operators that make it possible to write displacement components

in terms of mid-plane displacement on the upper surface. First, acting with (3.12) and (3.17) on (3.1), the Kirchoff plate equation can be rewritten in terms of the displacement components on the upper surface $x_3 = h$ as

$$D\Delta^2 u_i + 2\rho h \frac{\partial^2 u_i}{\partial t^2} = -h\left(1 + h^2\left(\frac{\nu+4}{6(1-\nu)}\frac{\partial^2}{\partial x_i^2} - \frac{5\nu}{6(1-\nu)}\frac{\partial^2}{\partial x_j^2}\right)\right)\frac{\partial P}{\partial x_i}, \tag{3.18}$$

and

$$D\Delta^2 u_3 + 2\rho h \frac{\partial^2 u_3}{\partial t^2} = \left(1 + h^2\frac{\nu}{2(1-\nu)}\frac{\partial^2}{\partial x_1^2}\right)P. \tag{3.19}$$

We may also apply the differantial operators (3.12) and (3.17) to the 'refined plate equations' given by (see, [26])

$$\begin{aligned} D\Delta^2 w + 2\rho h\left(1 + h^2\frac{7\nu-17}{15(1-\nu)}\Delta\right)\frac{\partial^2 w}{\partial t^2} - \left(1 - h^2\frac{8-3\nu}{10(1-\nu)}\Delta\right)Q_N - \\ - 2h\left(1 - h^2\frac{4+\nu}{30(1-\nu)}\Delta\right)\mathrm{div}_\Gamma \mathbf{Q}_T = 0. \end{aligned} \tag{3.20}$$

On doing so, the refined plate bending equation can be rewritten in terms of the displacement components on the upper surface $x_3 = h$

$$\begin{aligned} D\Delta^2 u_i + 2\rho h\left(1 + h^2\frac{7\nu-17}{15(1-\nu)}\Delta\right)\frac{\partial^2 u_i}{\partial t^2} = \\ \left(1 + h^2\left(\frac{\nu+4}{6(1-\nu)}\frac{\partial^2}{\partial x_i^2} - \frac{5\nu}{6(1-\nu)}\frac{\partial^2}{\partial x_j^2} - \frac{8-3\nu}{10(1-\nu)}\Delta\right)\right)\frac{\partial P}{\partial x_i}, i, j = 1, 2, i \neq j. \end{aligned} \tag{3.21}$$

and

$$D\Delta^2 u_3 + 2\rho h\left(1 + h^2\frac{7\nu-17}{15(1-\nu)}\Delta\right)\frac{\partial^2 u_3}{\partial t^2} = \left(1 - h^2\frac{4}{5}\Delta\right)P. \tag{3.22}$$

Thus, asymptotic expansion applied to displacements and stresses, the refined plate equation is obtained in terms of displacement components.

3.2. Dispersion Analysis

In this section, we will analyse dispersion relations as a preparation step for the construction of an asymptotic model. Starting with the wave equations (2.27), and substituting plane travelling solutions, in the form $e^{i(kx-\omega t)}$, we end up with

$$k^2 = \frac{\omega^2}{c_i^2}, \qquad i = 1, 2. \tag{3.23}$$

Equation (3.23) is known as the dispersion relation, which is a link between angular frequency ω and wave number k. This relation (3.23) means that waves with a given frequency must have a certain wave number, so it is important to characterization of waves. To analyse the natural vibration modes of a thin plate, we may take homogenous boundary conditions on the faces

$$\sigma_{31} = \sigma_{33} = 0 \quad \text{at} \quad x_3 = \pm h. \tag{3.24}$$

Expressing stress components in the given boundary conditions (3.24) in terms of the functions f and g defined by (2.33), in case of plate bending, for which we consider only antisymmetric modes, we obtain the following system of linear equations

$$\begin{aligned} AiK\alpha \cosh\alpha + B\left(K^2 - \Omega^2\right)^2 \cosh\beta = 0, \\ A\left(K^2 - \Omega^2\right)^2 \sinh\alpha - BiK\beta \cosh\beta = 0. \end{aligned} \tag{3.25}$$

In order for the solution of system of homogeneous equations (3.25), to exist, the determinant of coefficients must be zero. Equating the determinant of coefficients to zero in (3.25), we obtain the frequency equation

$$\left(K^2 - \Omega^2\right)^4 \frac{\sinh\alpha}{\alpha} \cosh\beta - \beta^2 K^2 \cosh\alpha \frac{\sinh\beta}{\beta} = 0. \tag{3.26}$$

The resulting equation (3.26) is the Rayleigh-Lamb frequency equation for the propagating waves with the antisymmetric modes in plate. To obtain dispersion relations for the problem that we introduce, we study the plane travelling wave solutions to the homogeneous forms of plate equations given in the previous section. The typical wavelength and time scale are defined as $L \sim k^{-1}$ and $T \sim \omega^{-1}$. First, we substitute the travelling wave solution $u_3 = U_3 e^{i(kx-\omega t)}$ into equations (3.1),(3.22) and (2.53) for $P = 0$, having

$$k^4 - \frac{3(1-\nu)}{2c_2^2 h^2}\omega^2 = 0, \tag{3.27}$$

$$k^4 - \frac{3(1-\nu)}{2c_2^2 h^2}\left(1 - h^2 \frac{7\nu - 17}{15(1-\nu)} k^2\right)\omega^2 = 0, \tag{3.28}$$

and

$$k^2 - \frac{1}{c_R^2}\omega^2 = 0. \tag{3.29}$$

Thus, we obtain the dispersion relations for Kirchoff plate equation (3.1), refined plate equation (3.22) and Rayleigh equation(2.53). Employing the scalings (2.29) in equations (3.27), (3.28) and (3.29) we get the nondimensional dispersion relations

$$K^4 - \frac{3(1-\nu)}{2}\Omega^2 = 0, \tag{3.30}$$

$$K^4 - \frac{3(1-\nu)}{2}\left(1 - \frac{7\nu - 17}{15(1-\nu)}K^2\right)\Omega^2 = 0, \tag{3.31}$$

and

$$K^2 - \frac{1}{v_R^2}\Omega^2 = 0, \tag{3.32}$$

corresponding to Kirchhoff plate bending (3.1), refined plate bending (3.22), and Rayleigh (2.53) equations, respectively. Here $v_R = \dfrac{c_R}{c_2}$ is the dimensionless Rayleigh wave speed. Having arrived at the required dispersion relations, we may suggest a 'simple' composite equation for dispersion relations based on (3.30) and (3.32), which is

$$K^4 - \frac{3(1-\nu)}{2}\Omega^2 - \frac{\Omega^4}{v_R^4} = 0. \tag{3.33}$$

The aim of writing equation (3.33) is to combine long-wave low-frequency and short-wave high-frequency one in a composite equation for different behaviors in different asymptotic approaches. It may easily be shown that this dispersion relation (3.33) contains both long–wave low–frequency and short–wave high–frequency limits. At the long–wave low–frequency limit, in which $\Omega \sim K^2 \ll 1$, we have

$$K^4 - \frac{3(1-\nu)}{2}\Omega^2 - \frac{K^8}{v_R^4} = 0, \tag{3.34}$$

the last term on the left-hand side is order of $O(\eta^2)$ and may be ignored at leading order, since $\eta = K \ll 1$. So, at leading order we arrive at the dispersion relation (3.30) from (3.33).

On the other hand, at the short–wave high–frequency limit, in which $\Omega \sim K \gg 1$,

we have

$$K^4 - \frac{3(1-\nu)}{2}K^2 - \frac{\Omega^4}{v_R^4} = 0, \tag{3.35}$$

we may neglect the middle term, which is of order $O(K^2)$, and arrive at the other shortened dispersion relation (3.32).

Next, by combining (3.31) and (3.32), we may propose a refined composite dispersion relation in the form

$$K^4 - \frac{3(1-\nu)}{2}\left(1-\delta K^2\right)\Omega^2 + \gamma K^2\Omega^2\left(K^2 - \frac{\Omega^2}{v_R^2}\right) = 0, \tag{3.36}$$

with

$$\delta = \frac{7\nu - 17}{15(1-\nu)}. \tag{3.37}$$

Here γ is a constant parameter to be found. To this end, we express (3.36) in the form

$$\left(1+\gamma\Omega^2\right)K^4 + \left(\frac{3(1-\nu)}{2}\delta - \gamma\frac{\Omega^2}{v_R^2}\right)\Omega^2K^2 - \frac{3(1-\nu)}{2}\Omega^2 = 0 \tag{3.38}$$

Considering (3.38) as a quadratic equation with respect to the variable K^2, we find its root to be

$$K^2 = \frac{1}{2\left(1+\gamma\Omega^2\right)}\left(-\left(\frac{3(1-\nu)}{2}\delta - \gamma\frac{\Omega^2}{v_R^2}\right)\Omega^2 + \sqrt{\left(\frac{3(1-\nu)}{2}\delta - \gamma\frac{\Omega^2}{v_R^2}\right)^2\Omega^4 + 6\left(1+\gamma\Omega^2\right)\Omega^2}\right). \tag{3.39}$$

By taking the square of both sides of (3.39), K^4 can be written as

$$K^4 = \frac{1}{4(1+\gamma\Omega^2)^2}\left[\left(2\left(\frac{3(1-\nu)}{2}\delta - \gamma\frac{\Omega^2}{v_R^2}\right)^2 + 6(1-\nu)\gamma\right)\Omega^4 + 6(1-\nu)\Omega^2 - \right. \tag{3.40}$$

$$\left. -2\left(\frac{3(1-\nu)}{2}\delta - \gamma\frac{\Omega^2}{v_R^2}\right)\Omega^2\sqrt{\left(\frac{3(1-\nu)}{2}\delta - \gamma\frac{\Omega^2}{v_R^2}\right)^2\Omega^4 + 6(1-\nu)(1+\gamma\Omega^2)\Omega^2}\right].$$

Equation (3.40) may be expanded at $\Omega \ll 1$ as follows:

$$K^4 = \frac{3(1-\nu)}{2}\Omega^2 \left(1 + \sqrt{\frac{3(1-\nu)}{2}}\delta\Omega + \left(\frac{3\delta^2(1-\nu)}{4} - \gamma\right)\Omega^2 + \dots\right). \tag{3.41}$$

Now, we require the last expansion (3.41) to coincide with the asymptotic expansion of Rayleigh–Lamb dispersion equation for the antisymmetric mode (3.26). Taking into account the analysis presented in [[26], section7.5, page 135.], we obtain

$$\begin{aligned} \gamma &= \frac{3\delta^2(1-\nu)}{4} - A_2 \\ &= \frac{-422 + 424\nu + 33\nu^2}{1050(-1+\nu)}. \end{aligned} \tag{3.42}$$

3.3. Numerical Results

In this section numerical values of the solutions are illustrated. We may obtain the numerical results for small and large values of Ω in dispersion relations (3.30), (3.31),(3.32), (3.33), (3.36) and (3.26), corresponding to low and high–frequency limits. Table 1 shows the numerical results for the dispersion relations in the case of Poisson's ratio $\nu = 0.25$ for which the positive root of Rayleigh equation (3.26) is given, approximately, by $v_R = 0.9194$. The first two columns of Table 1 corresponds to the Kirchoff and refined plate limits and therefore only the results of the smaller values of Ω are presented in these two columns. Likewise, third column correspond the high frequency limit, that is the Rayleigh equation, and thus only the numerics of large Ω is given.

Ω	Kirchhoff plate dispersion relation (3.30)	Refined Plate dispersion relation (3.31)	Rayleigh wave asymptote (3.32)	Composite dispersion relation (3.33)	Refined composite dispersion relation (3.36)	Rayleigh–Lamb dispersion relation (3.26)
0.1	0.3256	0.3375		0.3348	0.3372	0.3372
0.2	0.4605	0.4947		0.4869	0.4929	0.4930
0.3	0.5640	0.6278		0.6130	0.6229	0.6233
0.4	0.6513	0.7506		0.7275	0.7409	0.7418
0.5	0.7282	0.8684		0.8357	0.8519	0.8537
1.	1.029	1.438		1.343	1.363	1.373
1.5	1.261	2.013		1.845	1.858	1.873
2	1.456	2.600		2.354	2.360	2.374
2.5			2.719	2.871	2.872	2.880
3			3.262	3.394	3.392	3.391
4			4.350	4.453	4.448	4.428
5			5.438	5.522	5.517	5.482
6			6.525	6.596	6.591	6.550
8			8.701	8.755	8.750	8.707
10			10.87	10.91	10.91	10.87
11			11.96	12.00	12.00	11.96
12			13.05	13.08	13.08	13.05

Table 1. Dispersion relations.

Visualizing the data shown in Table 1 obtained from dispersion equations (3.30), (3.31), (3.32), (3.33), (3.36) and (3.26), it is easier to compare the behavior of the composite equation in the limiting cases corresponding to the plate bending and Rayleigh equations.

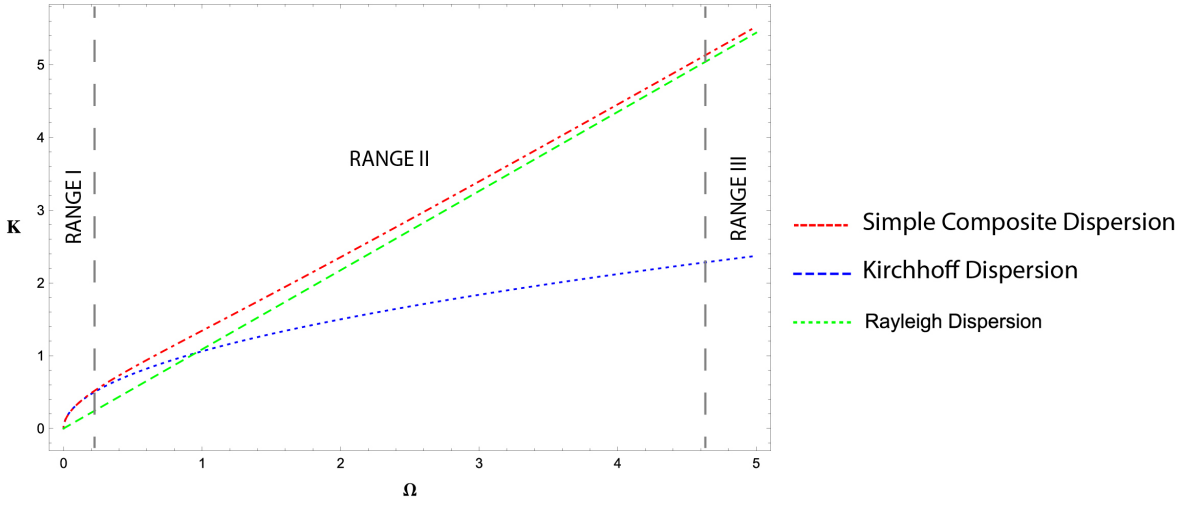

Figure 3.2. Dispersion curves for Kirchhoff equation (3.30), composite equation (3.33), and Rayleigh wave (3.32).

Figure 3.2 displays dispersion curves for Kirchoff plate (3.30), simple composite equation(3.33) and Rayleigh wave (3.32) plotted by blue, red and green lines, respectively. Graphic material is supported by the numerical data in columns 1, 3 and 4 in Table 1. As shown in the graph, the composite dispersion curve displays the same behavior as the Rayleigh limit for large values of Ω and the plate limit for the small values of the Ω.

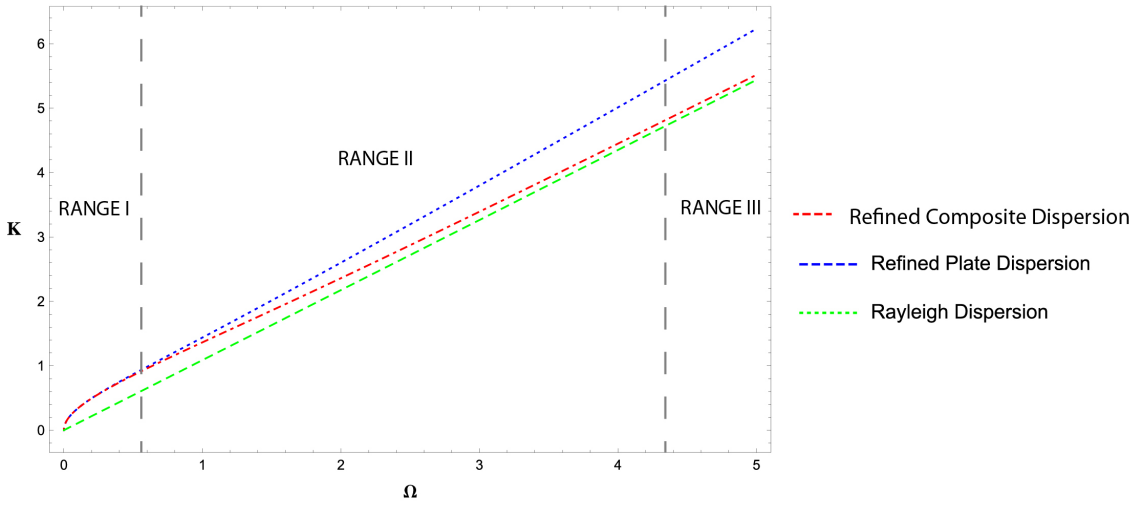

Figure 3.3. Dispersion curves for refined plate equation (3.31), refined composite equation (3.36), and Rayleigh wave (3.32).

The dispersion curves plotted in Figure 3.3 by blue–dashed, red–dashdotted lines, correspond to the refined plate (3.31) and composite equation (3.36), respectively; see also columns 2 and 5 in Table 1. As might be expected, the deviation between the predictions of composite relation (3.33) and its refined form (3.36) is more substantial at relatively low frequencies, while it is rather minor at the high-frequency limit. The obvious reason is that both composite relations utilise the same Rayleigh wave

asymptote.

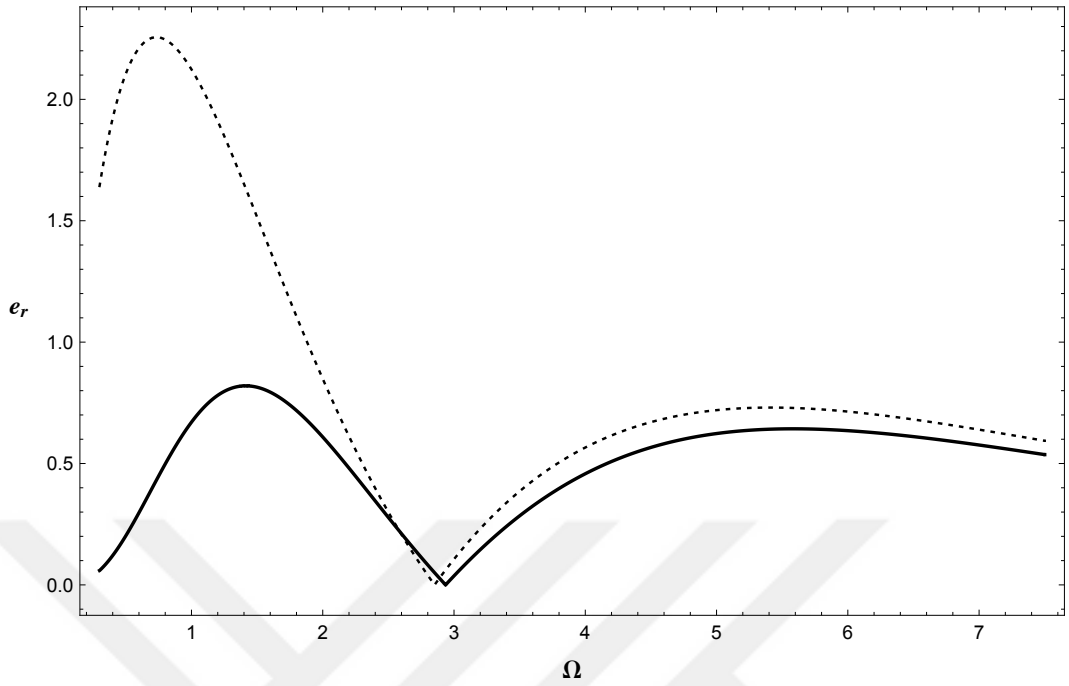

Figure 3.4. Relative error for composite equation (3.33) and refined composite equation (3.36).

The accuracy of composite relations (3.33) and (3.36) is tested in Figure 3.4 by comparison with the numerical solution of the Rayleigh–Lamb equation, see (3.26). Computations for the latter are also presented in the last column of the Table 1. The relative error is plotted with the following expression

$$e_r = \left| \frac{K_{RL} - K}{K_{RL}} \right| \times 100\%, \tag{3.43}$$

where K_{RL} denotes the associated Rayleigh–Lamb root. It is depicted with dashed and solid lines for K found from composite relations (3.33) and (3.36), respectively. The curves corresponding to composite relations meet that for the Rayleigh–Lamb equation at $\Omega \approx 3$. This reduces the approximation error over the intermediate frequency range, which is of main concern from the very beginning. To the left of $\Omega = 3$, the refined relation has a clear advantage, while to the right of it the difference between (3.33) and (3.36) is not that considerable.

3.4. Construction of the Composite Equation For Vertical Displacement Component

In this section our aim is establish $2D$ composite wave models containing plate bending and Rayleigh wave equations as their asymptotic long–wave low–frequency and short–wave high–frequency limits corresponding to (2.34) and (2.41), respectively. At the same time, we do not expect an uniform asymptotic behaviour since the intermediate domain

$$L \sim h \quad \text{and} \quad T \sim \sqrt{\frac{\rho}{E}}h \tag{3.44}$$

is not addressed. However it should be emphasised that two incorporated limits approximate the dominant part of the overall dynamic response related to the zone of intensive flexural vibration and vicinities of Rayleigh wave front on plate faces, in doing so, the rest of the response consists of low amplitude vibration.
Acting (3.12) on (3.1), we obtain Kirchoff plate bending equation in terms of u_3 at leading order

$$D\Delta^2 u_3 + 2\rho h\frac{\partial^2 u_3}{\partial t^2} = P, \tag{3.45}$$

along the upper surface $x_3 = h$. Starting with (3.45) and (2.53), we obtain a composite asymptotic equation for vertical displacement u_3 along the faces $x_3 = \pm h$

$$D\Delta^2 u_3 - \frac{D}{c_R^2}\Delta\frac{\partial^2 u_3}{\partial t^2} + 2\rho h\frac{\partial^2 u_3}{\partial t^2} = \left(1 - h^3\frac{k_1\left(1-k_2^2\right)}{3B(1-\nu)}\sqrt{-\Delta}\Delta\right)P. \tag{3.46}$$

This simplest composite equation (3.46) can easily be reduced the original shortened equations at the long–wave low–frequency and short–wave high–frequency limits. In order to show this, let us start by scaling the original variables as

$$x_i = \xi_i L, \quad i = 1, 2, \text{ and } \quad t = T\tau. \tag{3.47}$$

Then, for long–wave low–frequency limit assuming that $\eta = \dfrac{h}{L} \ll 1$ and $T = \dfrac{L}{\eta c_2}$ (see (2.34)), we have

$$\frac{D}{L^4}\left(\Delta_*^2 u_3 - \eta^2 \frac{1}{v_R^2}\Delta_* \frac{\partial^2 u_3}{\partial \tau^2} + \frac{3(1-\nu)}{2}\frac{\partial^2 u_3}{\partial \tau^2}\right) = \left(1 + \eta^3 \frac{k_1(1-k_2^2)}{3B(1-\nu)}\sqrt{-\Delta_*}\Delta_*\right) P, \tag{3.48}$$

where $\Delta_* = \dfrac{\partial^2}{\partial \xi_i^2} + \dfrac{\partial^2}{\partial \xi_j^2}$. Dividing both side of (3.48) by $\dfrac{L^4}{D}$ and applying Δ_*, we get

$$\left(\Delta_* - \eta^2 \frac{1}{v_R^2}\Delta_* \frac{\partial^2 u_3}{\partial \tau^2}\right)\Delta_* u_3 + \frac{3(1-\nu)}{2}\frac{\partial^2 u_3}{\partial \tau^2} = \left(1 + \eta^3 \frac{k_1(1-k_2^2)}{3B(1-\nu)}\sqrt{-\Delta_*}\Delta_*\right)\frac{PL^4}{D}, \tag{3.49}$$

It is, now, clear that, at leading order, that is ignoring terms of order $O(\eta^2)$, (3.49) coincides with Kirchoff plate equation (3.45) when written in nondimensional variables.

Now let $\eta = \dfrac{h}{L} \gg 1$ and $T = \dfrac{L}{c_R}$ (see (2.41)), resulting equation is

$$\frac{D}{L^4}\left(\Delta_*^2 u_3 - \Delta_* \frac{\partial^2 u_3}{\partial \tau^2} + \eta^{-2} v_R^2 \frac{3(1-\nu)}{2}\frac{\partial^2 u_3}{\partial \tau^2}\right) = \left(1 + \eta^3 \frac{k_1(1-k_2^2)}{3B(1-\nu)}\sqrt{-\Delta_*}\Delta_*\right) P, \tag{3.50}$$

$$\Delta_*\left(\Delta_* - \Delta_* \frac{\partial^2}{\partial \tau^2}\right) u_3 + \eta^{-2} v_R^2 \frac{3(1-\nu)}{2}\frac{\partial^2 u_3}{\partial \tau^2} = \left(\eta^{-3} + \frac{k_1(1-k_2^2)}{3B(1-\nu)}\sqrt{-\Delta_*}\Delta_*\right)\frac{PL^4\eta^3}{D}. \tag{3.51}$$

In (3.51) neglecting $O(\eta^{-2})$ terms and cancelling out the operator Δ_*, we obtain short–wave high–frequency limit for simple composite model, which coincides with (2.53).

Next, we implement the refined plate equation (3.20) and proceed in the same manner as above. Then, a more sophisticated composite equation for vertical displacement may be presented as

$$D\left(1 - h^2 \frac{\gamma}{c_2^2}\frac{\partial^2}{\partial t^2}\right)\Delta^2 u_3 + 2\rho h\left(1 + h^2\delta\Delta + h^4 \frac{2\gamma}{3(1-\nu)c_R^2}\Delta\frac{\partial^2}{\partial t^2}\right)\frac{\partial^2 u_3}{\partial t^2} = \\ = \left(1 - h^2\frac{4}{5}\Delta + \frac{h^5}{c_2^2}\frac{\gamma k_1(1-k_2^2)}{3B(1-\nu)c_2^2}\sqrt{-\Delta}\Delta\frac{\partial^2}{\partial t^2}\right) P. \tag{3.52}$$

Again, it may be shown that equation (3.52) is reduced to its original shortened forms at the long-wave low-frequency and Rayleigh wave limits using proper scalings.

In particular, at low-frequency limit, (3.52), written in terms of the dimensionless variables (4.6), takes the form

$$\left(1-\eta^4\gamma\frac{\partial^2}{\partial\tau^2}\right)\Delta_*^2u_3+\frac{3(1-\nu)}{2}\left(1+\eta^2\delta\Delta_*+\eta^6\frac{2\gamma c_2^2}{3(1-\nu)c_R^2}\Delta_*\frac{\partial^2}{\partial\tau^2}\right)\frac{\partial^2u_3}{\partial\tau^2}= \\ =\left(1-\eta^2\frac{4}{5}\Delta_*+\eta^7\frac{\gamma k_1(1-k_2^2)}{3B(1-\nu)}\sqrt{-\Delta_*}\Delta_*\frac{\partial^2}{\partial\tau^2}\right)\frac{PL^4}{D}. \tag{3.53}$$

This time let us keep $O(\eta^2)$ terms, neglecting all the smaller ones, to obtain

$$\Delta_*^2u_3+\frac{3(1-\nu)}{2}\left(1+\eta^2\delta\Delta_*\right)\frac{\partial^2u_3}{\partial\tau^2}=\left(1-\eta^2\frac{4}{5}\Delta_*\right)\frac{PL^4}{D}. \tag{3.54}$$

This equation is identical to refined plate equation (3.20) rewritten in dimensionless variables. Now we get from (3.53) at the Rayleigh wave limit

$$\left(\eta^{-2}-\gamma\frac{c_R^2}{c_2^2}\frac{\partial^2}{\partial\tau^2}\right)\Delta_*^2u_3+\frac{c_R^2}{c_2^2}\frac{3(1-\nu)}{2}\left(\eta^{-4}+\eta^{-2}\delta\Delta_*+\frac{2\gamma}{3(1-\nu)}\Delta_*\frac{\partial^2}{\partial\tau^2}\right)\frac{\partial^2u_3}{\partial\tau^2}= \\ =\left(\eta^{-5}-\eta^{-3}\frac{4}{5}\Delta_*+\frac{\gamma k_1(1-k_2^2)}{3B(1-\nu)}v_R^2\sqrt{-\Delta_*}\Delta_*\frac{\partial^2}{\partial\tau^2}\right)\frac{PL^4\eta^3}{D}. \tag{3.55}$$

At leading order, the latter becomes

$$\Delta_*\frac{\partial^2}{\partial\tau^2}\left(\Delta_*-\frac{\partial^2}{\partial\tau^2}\right)u_3=-\frac{L^4\eta^3}{D}\frac{k_1(1-k_2^2)}{3B(1-\nu)}\sqrt{-\Delta_*}\Delta_*\frac{\partial^2P}{\partial\tau^2}. \tag{3.56}$$

Finally, cancelling out operator $\Delta_*\dfrac{\partial^2}{\partial\tau^2}$, we have Rayleigh wave equation (2.53) presented in a dimensionless form.

As might be expected, the dispersion relation corresponding to refined composite equation (3.52) is the same as (3.36).

3.5. An Illustrative Example

As an example, we consider the effect of the surface loads, see Figure.2.1, in the form of plane time-harmonic travelling waves, for which $P=P_0e^{i(k_0x_1-\omega t)}$, where $k_0=k_0(\omega)$ is a given function of angular frequency ω. Let us search for

the solution to the differential equations in Sections 3.1 and 2.7 also in the form of a plane travelling wave, i.e. take $u_3 = A\dfrac{hP_0}{\mu}e^{i(k_0x_1-\omega t)}$, where A is normalized amplitude.

First, insert u_3 and P into the composite equation (3.46) and its shortened limiting forms (3.19) and (2.53). Then, we have, respectively,

$$A = \frac{3(1-\nu)B + k_1(1-k_2^2)K_0^3}{4B(K_0^4 - \frac{1}{v_R^2}K_0^2\Omega^2 - \frac{3(1-\nu)}{2}\Omega^2)}. \tag{3.57}$$

$$A = \frac{3(1-\nu)}{4}\frac{1}{K_0^4 - \dfrac{3(1-\nu)}{2}\Omega^2}, \tag{3.58}$$

and

$$A = \frac{k_1(1-k_2^2)}{4B}\frac{K_0}{K_0^2 - \Omega^2/v_R^2}, \tag{3.59}$$

where, as before, $\Omega = \omega/c_2$ and $K_0 = k_0h$.

Next, insert u_3 and P into refined composite and plate equations (3.52) and (3.22) to obtain

$$A = \frac{1}{20B}\frac{3(1-\nu)(5+4K_0^2)B + 5k_1(1-k_2^2)\gamma K_0^3\Omega^2}{(1+\gamma\Omega^2)\,K_0^4 - \left(\frac{3(1-\nu)}{2} - \frac{7\nu-17}{10}K_0^2 + \frac{\gamma}{v_R^2}K_0^2\Omega^2\right)\Omega^2}. \tag{3.60}$$

and

$$A = \frac{3(1-\nu)}{20}\frac{5+4K_0^2}{K_0^4 - \frac{3(1-\nu)}{2}\,(1-\delta K_0^2)\,\Omega^2}, \tag{3.61}$$

or, multiplying numerator and denominator by $5-4K_0$ in (3.61),

$$A = \frac{3(1-\nu)}{20}\frac{25-16K_0^4}{5K_0^4 - \frac{15(1-\nu)}{2}\Omega^2 - \frac{5}{2}(1+\nu)K_0^2\Omega^2 - 4K_0^6 - 6(1-\nu)\delta K_0^4\Omega^2}, \tag{3.62}$$

This formula, to within higher-order terms, coincides with (3.109), the long-wave low-frequency expansion of exact solution (3.107) at $K = K_0$. Also, expression (3.59) is the same as Rayleigh wave limit (3.110) at $K = K_0$ due to the identity

$4B = v_R R'(v_R)$.

Numerical data are given Figures 3.5–3.7 and Table 2 for $\nu = 0.25$, $v_R = 0.9194$, and $\varepsilon = 0.02$.

Ω	Kirchhoff equation (3.58)	Refined Plate equation (3.61)	Rayleigh wave equation (3.59)	Composite equation (3.57)	Refined Composite equation (3.60)	Plane elasticity equations (3.107)
0.1	-50.5804	-50.2571		-49.9961	-50.2571	-50.2027
0.2	-13.1013	-12.7541		-12.5158	-12.7544	-12.7031
0.3	-6.19535	-5.80486		-5.591	-5.80606	-5.75931
0.4	-3.82774	-3.36786		-3.17994	-3.37107	-3.32969
0.5	-2.8045	-2.23504		-2.07423	-2.2416	-2.20589
1	3.39117	-0.685338		-0.666011	-0.731965	-0.71589
1.5	0.140492	-0.35926		-0.468618	-0.476211	-0.454868
2	0.0348212	-0.225405		-0.437286	-0.42102	-0.381079
2.5			-1.66994	-0.442851	-0.421085	-0.365705
3			-1.39161	-0.454562	-0.434849	-0.375865
4			-1.04371	-0.467465	-0.456193	-0.426026
5			-0.834968	-0.46161	-0.456402	-0.474053
6			-0.695806	-0.443547	-0.441541	-0.492547
8			-0.521855	-0.394237	-0.394421	-0.450213
10			-0.417484	-0.345513	-0.346039	-0.379392
11			-0.379531	-0.323708	-0.324228	-0.34778
12			-0.347903	-0.303819	-0.304299	-0.320075

Table 2. Displacement amplitude for Kirchoff equation (3.58), Refined Plate equation (3.61), Rayleigh wave equation (3.59), Composite equation (3.57), Refined composite equation (3.60), Plane elasticity equation (3.107)

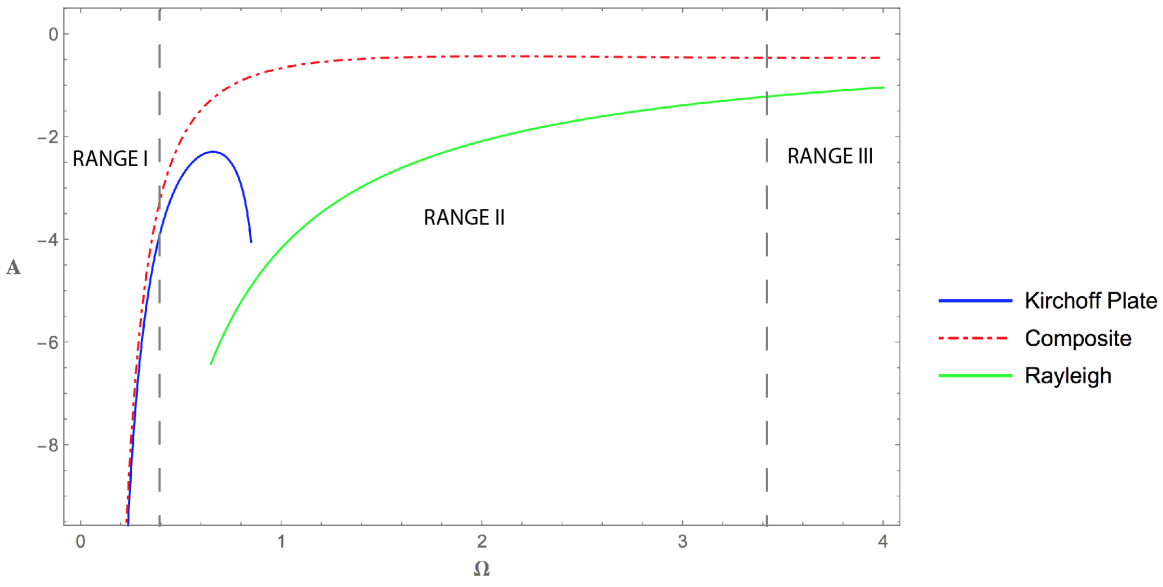

Figure 3.5. Displacement amplitude for composite equation (3.57), Kirchhoff equation (3.58), and Rayleigh wave equation (3.59).

In Figure 3.5 the solutions of composite equation (3.57) is plotted by the red dotted and dashed line, along with those of Kirchoff plate equation (3.58) and Rayleigh wave model (3.59) are plotted by the blue and green solid line, respectively. In

Range I, the Kirchoff plate displacement curve (3.58) and the composite displacement curves (3.57) are matching, as expected, for small values of Ω. From Range II it can easily be said that the composite displacement curve (3.57) approaches the Rayleigh wave model curve (3.59).

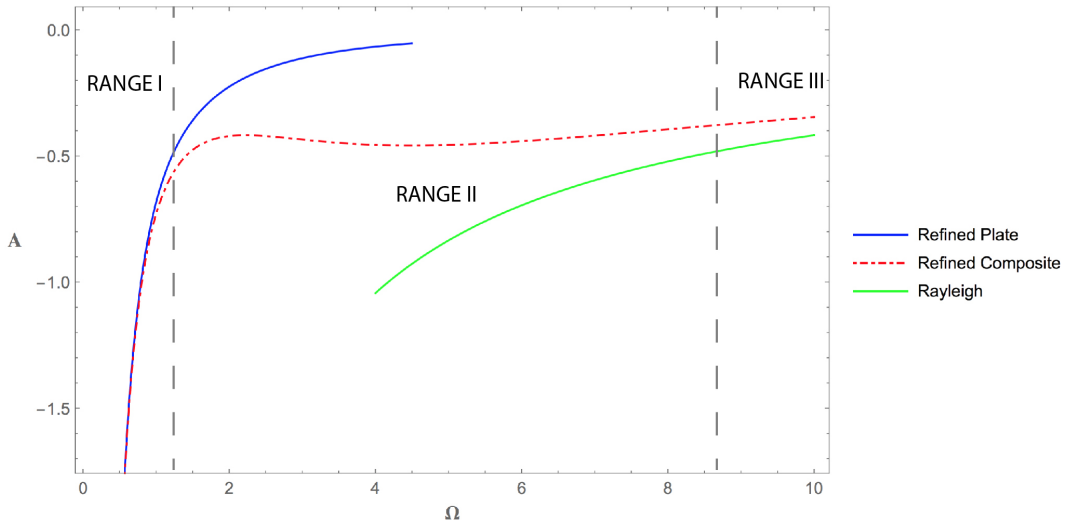

Figure 3.6. Displacement amplitude for refined composite equation (3.60), refined plate equation (3.61), and Rayleigh wave equation (3.59).

It is possible to make similar comparison between (3.60), (3.61) and (3.59). In Figure 3.6 the solutions of refined composite equation (3.60), refined plate equation (3.61) and Rayleigh equation (3.59) are plotted by red dotted and dashed line, blue and green solid lines, respectively. In Range I, refined composite displacement curve and refined plate curve are well matched. In Range III, Rayleigh curve approaches refined composite displacement curve, as expected. It is interesting that behaviours of the solutions of the Kirchhoff and refined plate equations appear to be quite different over the intermediate frequency range in both Figure 3.5 and Figure 3.6.

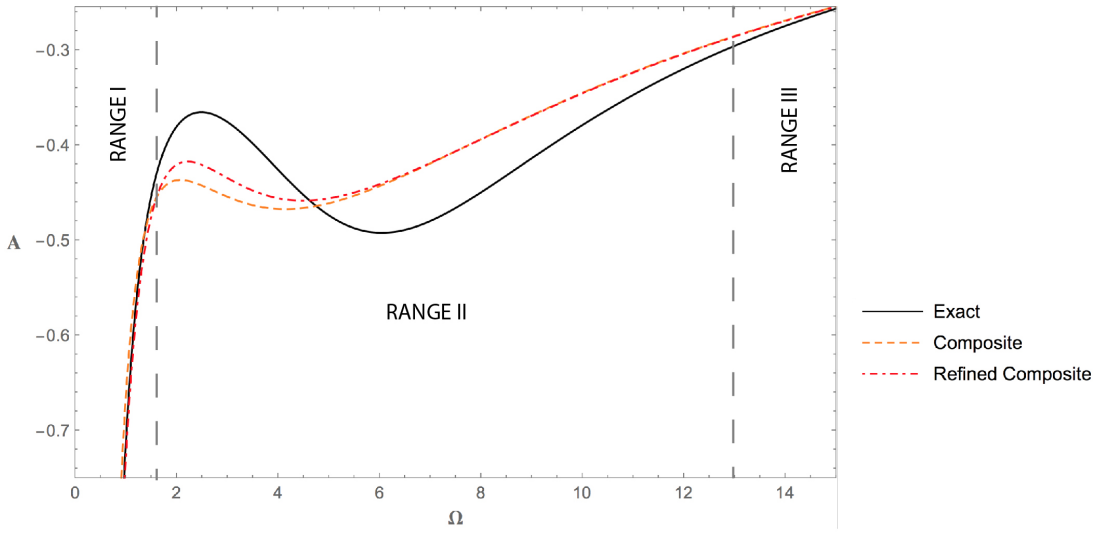

Figure 3.7. Displacement amplitude for composite equation (3.57), refined composite equation (3.60), and plane elasticity (3.107).

In the last Figure 3.7, the solution of the composite equation is compared with the exact solution of the associated problem in plane elasticity (3.107), see also the last column of the Table 2. Figure 3.7 and the Table 2 indicate a reasonable accuracy of the composite equations also over the intermediate frequency range. As for the dispersion curves in Section 3.2, the main improvement brought by the refined composite equation is observed at relatively low frequencies.

3.6. Section Summary

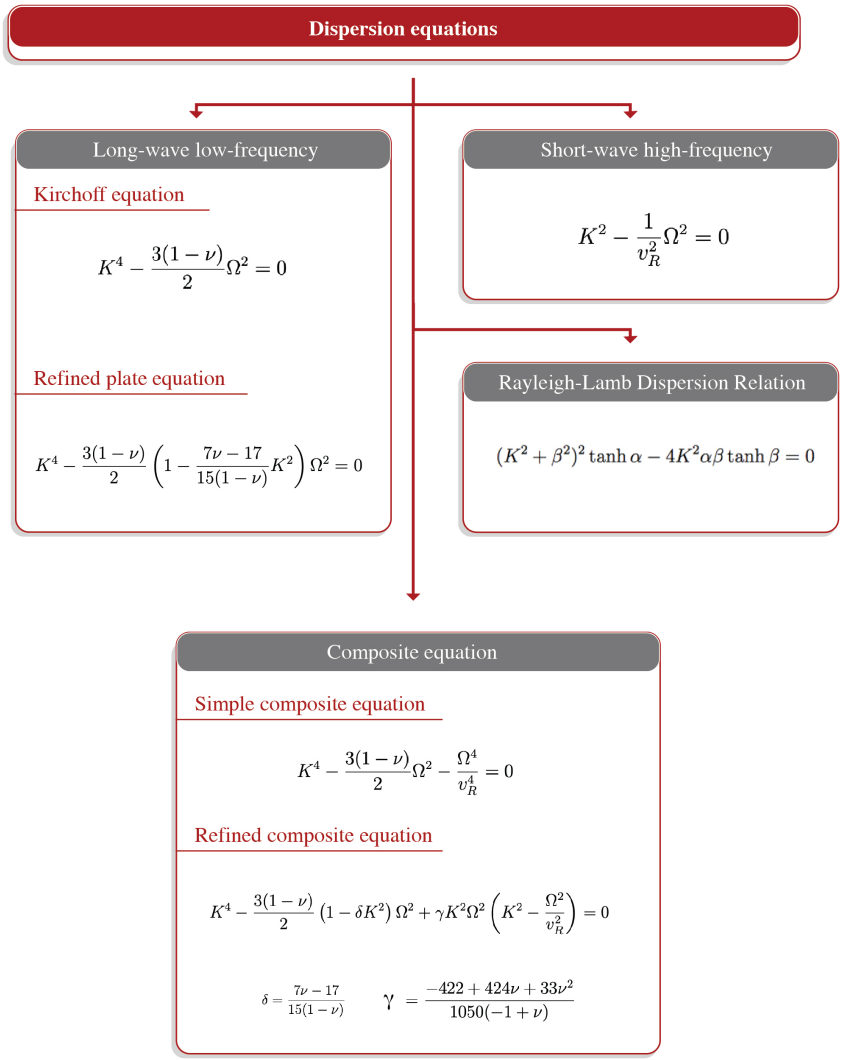

Figure 3.8. Dispersion Equations

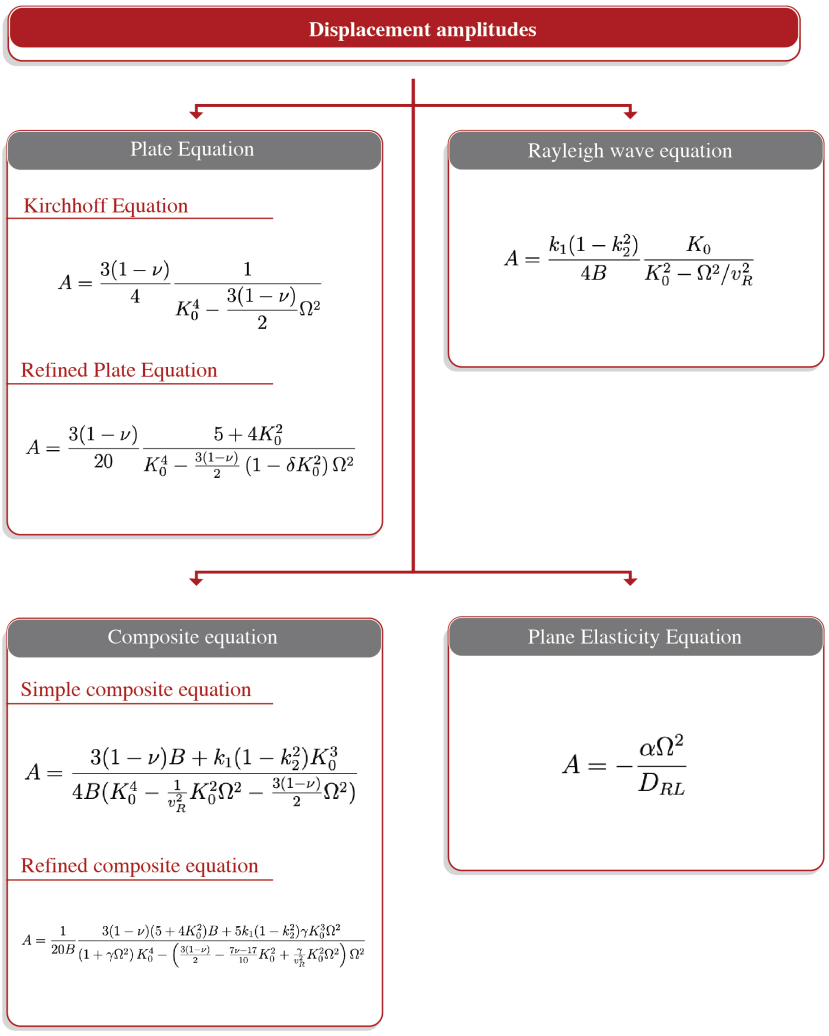

Figure 3.9. Displacement Amplitudes

3.7. Construction of the Composite Equation For Horizontal Displacement Component

In this section our aim is establish a composite wave model containing plate bending and Rayleigh wave equation in terms of horizontal displacement component u_1. We will follow smilar procedure as we did for vertical displacement component u_3 in previous section 3.4. From the equation(3.21) taking $i = 1, j = 2$, we may write refined plate equation in terms of horizontal displacement component u_1 as

$$D\Delta^2 u_1 + 2\rho h\left(1 + h^2\frac{7\nu - 17}{15(1-\nu)}\Delta\right)\frac{\partial^2 u_1}{\partial t^2} = \left(1 + h^2\left(\frac{\nu+4}{6(1-\nu)}\frac{\partial^2}{\partial x_1^2} - \frac{5\nu}{6(1-\nu)}\frac{\partial^2}{\partial x_2^2} - \frac{8-3\nu}{10(1-\nu)}\Delta\right)\right)\frac{\partial P}{\partial x_1}, \tag{3.63}$$

with $\Delta = \dfrac{\partial^2}{\partial x_1^2}$. Since the problem is independent of the horizontal coordinate x_2, we take $\dfrac{\partial}{\partial x_2} = 0$ in (3.63) to get

$$D\Delta^2 u_1 + 2\rho h\left(1 + h^2\frac{7\nu - 17}{15(1-\nu)}\Delta\right)\frac{\partial^2 u_1}{\partial t^2} = -h\left(1 - h^2\frac{2-7\nu}{15(1-\nu)}\frac{\partial^2}{\partial x_1^2}\right)\frac{\partial P}{\partial x_1}. \tag{3.64}$$

Taking $i = 1$ on (2.52), we get

$$\Delta u_1 - \frac{1}{c_R^2}\frac{\partial^2 u_1}{\partial t^2} = -\frac{1 - k_2^4}{8\mu B}\frac{\partial P}{\partial x_1}. \tag{3.65}$$

We may suggest a composite equation by adding terms into refined plate equation (3.64) to balance Rayleigh terms from (3.65). Thus, we may write the following composite equation with unknown coefficients θ and γ

$$D\frac{\partial^4 u_1}{\partial x_1^4} + 2\rho h\left(1 + h^2\frac{7\nu - 17}{15(1-\nu)}\frac{\partial^2}{\partial x_1^2}\right)\frac{\partial^2 u_1}{\partial t^2} + \theta\frac{\partial^4 u_1}{\partial t^4} = -h\left(1 - h^2\frac{2-7\nu}{15(1-\nu)}\frac{\partial^2}{\partial x_1^2} + \gamma\frac{\partial^2}{\partial t^2}\right)\frac{\partial P}{\partial x_1}. \tag{3.66}$$

Multiplying Rayleigh equation (3.65) by D and taking derivative with respect to x_1 twice, we get

$$D\frac{\partial^4 u_1}{\partial x_1^4} - \frac{D}{c_R^2}\frac{\partial^4 u_1}{\partial x_1^2 \partial t^2} = \frac{D}{4}\frac{c_R^2}{c_2^2}\frac{1 + k_2^2}{2\mu B}\frac{\partial^3 P}{\partial x_1^3}. \tag{3.67}$$

Now, it is possible to find the unknown coefficients θ and γ by comparing terms of (3.66) and (3.67). At short–wave high–frequency limit since we have the Rayleigh wave equation the following relation holds:

$$\frac{\partial^2}{\partial x_1^2} = \frac{1}{c_R^2}\frac{\partial^2}{\partial t^2}. \tag{3.68}$$

If we take the third and fourth terms of the left side of the composite equation (3.66), they must be balanced with the second term of the left side of the Rayleigh equation (3.67)

$$2\rho h^3 \frac{7\nu - 17}{15(1-\nu)}\frac{\partial^4 u_1}{\partial x_1^2 \partial t^2} + \theta \frac{\partial^4 u_1}{\partial t^4} = -\frac{D}{c_R^2}\frac{\partial^4 u_1}{\partial x_1^2 \partial t^2}. \tag{3.69}$$

Using (3.68) in (3.69) at long–wave low–frequency limit, we get

$$2\rho h^3 \frac{7\nu - 17}{15(1-\nu)}\frac{\partial^4 u_1}{\partial x_1^2 \partial t^2} + \theta c_R^2 \frac{\partial^4 u_1}{\partial x_1^2 \partial t^2} = -\frac{D}{c_R^2}\frac{\partial u_1}{\partial x_1^2 \partial t^2}. \tag{3.70}$$

From (3.70) we obtain the unknown coefficient θ as

$$\theta = -\frac{D}{c_R^4} - \frac{2\rho h^3}{c_R^2}\frac{7\nu - 17}{15(1-\nu)}. \tag{3.71}$$

The remaining coefficient γ may be found in similar manner. To this end, we balance second and third terms of the right side of composite equation (3.66) and the term in the right side of the Rayleigh equation (3.67) giving

$$h^3 \frac{2 - 7\nu}{15(1-\nu)}\frac{\partial^3 P}{\partial x_1^3} - h\gamma \frac{\partial^3 P}{\partial x_1 \partial t^2} = D\frac{c_R^2}{c_2^2}\frac{1 + k_2^2}{8\mu B}\frac{\partial^3 P}{\partial x_1^3}. \tag{3.72}$$

Using (3.68) in (3.72) at short–wave high–frequency limit, we get

$$h^3 \frac{2 - 7\nu}{15(1-\nu)}\frac{\partial^3 P}{\partial x_1^3} - hc_R^2\gamma \frac{\partial^3 P}{\partial x_1^3} = D\frac{c_R^2}{c_2^2}\frac{1 + k_2^2}{8\mu B}\frac{\partial^3 P}{\partial x_1^3}. \tag{3.73}$$

From (3.73) we obtain γ as

$$\gamma = \frac{h^2}{c_R^2}\frac{2 - 7\nu}{15(1-\nu)} - \frac{D}{hc_R^2}\frac{1 + k_2^2}{8\mu B}. \tag{3.74}$$

Now that we obtain the coefficients θ and γ, using (3.71) and (3.74) we may rewrite the composite equation(3.66)

$$D\frac{\partial^4 u_1}{\partial x_1^4}+2\rho h\left(1+h^2\frac{7\nu-17}{15(1-\nu)}\frac{\partial^2 u_1}{\partial x_1^2}\right)\frac{\partial^2 u_1}{\partial t^2}-\left(\frac{D}{c_R^4}\frac{2\rho h^3}{c_R^2}\frac{7\nu-17}{15(1-\nu)}\right)\frac{\partial^4 u_1}{\partial t^4}= \quad (3.75)$$
$$-h\left(1-h^2\frac{2-7\nu}{15(1-\nu)}\frac{\partial^2}{\partial x_1^2}+\left(\frac{h^2}{c_R^2}\frac{2-7\nu}{15(1-\nu)}-\frac{D}{hc_2^2}\frac{1+k_2^2}{8\mu B}\right)\frac{\partial^2}{\partial t^2}\right)\frac{\partial P}{\partial x_1}.$$

Multiplying both sides of (3.75) by $\frac{h^4}{D}$ and writing in terms of dimensionless variables, we get

$$\frac{\partial^4 u_1}{\partial \xi^4}+\left(\frac{3(1-\nu)}{2}+h^2\frac{7\nu-17}{10}\frac{\partial^2 u_1}{\partial \xi^2}\right)\frac{\partial^2 u}{\partial \tau^2}-\left(\frac{1}{v_R^4}+\frac{7\nu-17}{10v_R^2}\right)\frac{\partial^4 u_1}{\partial \tau^4}= \quad (3.76)$$
$$-\frac{h}{\mu}\left(\frac{3(1-\nu)}{4}-\frac{2-7\nu}{20}\frac{\partial^2}{\partial \xi^2}+\left(\frac{2-7\nu}{20v_R^2}-\frac{1+k_2^2}{8B}\right)\frac{\partial^2}{\partial \tau^2}\right)\frac{\partial P}{\partial \xi_1},$$

where $V_R=\frac{c_R}{c_2}$ is the dimensionless Rayleigh wave speed.

3.8. Dispersion analysis

In this section, we study plane travelling wave solutions to the homogenous form of composite equation (3.75), refined plate equation (3.64) and Rayleigh equation (3.65)($P=0$) given, respectively by

$$D\frac{\partial^4 u_1}{\partial x_1^4}+2\rho h\left(1+h^2\frac{7\nu-17}{15(1-\nu)}\frac{\partial^2 u}{\partial x_1^2}\right)\frac{\partial^2 u}{\partial t^2}-\left(\frac{D}{c_R^4}\frac{2\rho h^3}{c_R^2}\frac{7\nu-17}{15(1-\nu)}\right)\frac{\partial^4 u_1}{\partial t^4}=0, \quad (3.77)$$

$$D\frac{\partial^4 u_1}{\partial x_1^4}+2\rho h\left(1+h^2\frac{7\nu-17}{15(1-\nu)}\frac{\partial^2}{\partial x_1^2}\right)\frac{\partial^2 u_1}{\partial t^2}=0, \quad (3.78)$$

$$\frac{\partial^2 u_1}{\partial x_1^2}-\frac{1}{{c_R}^2}\frac{\partial^2 u_1}{\partial t^2}=0. \quad (3.79)$$

We are going to sought for the solutions of (3.77),(3.78) and (3.79) in the form

$$u_1=\frac{ihP_0A}{\mu}e^{i(\omega t-kx_1)}. \quad (3.80)$$

Here, ω is angular frequency and k is wavenumber.

Inserting (3.80) into (3.77), (3.78) and (3.79), we get

$$K^4 - \left(\frac{3(1-\nu)}{2} - \frac{7\nu-17}{10}K^2\right)\Omega^2 - \left(\frac{1}{s^4} - \frac{7\nu-17}{10v_R^2}\right)\Omega^4 = 0, \tag{3.81}$$

$$K^4 - \left(\frac{3(1-\nu)}{2} - \frac{7\nu-17}{10}K^2\right)\Omega^2 = 0, \tag{3.82}$$

$$K^2 - \frac{\Omega^2}{s^2} = 0, \tag{3.83}$$

where

$$K = kh \quad \text{and} \quad \Omega = \frac{\omega h}{c_2}, \tag{3.84}$$

are dimensionless and wavenumber and angular frequency respectively.

From composite dispersion relation (3.81), refined plate dispersion relation (3.82) and Rayleigh dispersion relation (3.83) we may express K as

$$K = \sqrt{-\frac{7\nu-17}{20}\Omega^2 + \frac{1}{2}\sqrt{\frac{(7\nu-17)^2\Omega^4}{100} + 6(1-\nu)\Omega^2 + 4\left(\frac{1}{v_R^4} + \frac{7\nu-17}{10v_R^2}\right)\Omega^4}}, \tag{3.85}$$

$$K = \sqrt{-\frac{7\nu-17}{20}\Omega^2 + \frac{1}{2}\sqrt{\frac{(7\nu-17)^2\Omega^4}{100} + 6(1-\nu)\Omega^2}}, \tag{3.86}$$

$$K = \frac{\Omega}{v_R} \tag{3.87}$$

Numerical results are presented in Figure 3.10 for the Poisson ratio $\nu = 0.25$ for which the positive root of the Rayleigh equation is given, approximately, by $v_R = 0.9194$. Figure 3.10 displays the dispersion curves for refined refined plate equation (3.86), composite equation (3.85), and Rayleigh wave (3.87) plotted by dashed blue line, red solid line, and dotted green line, respectively.

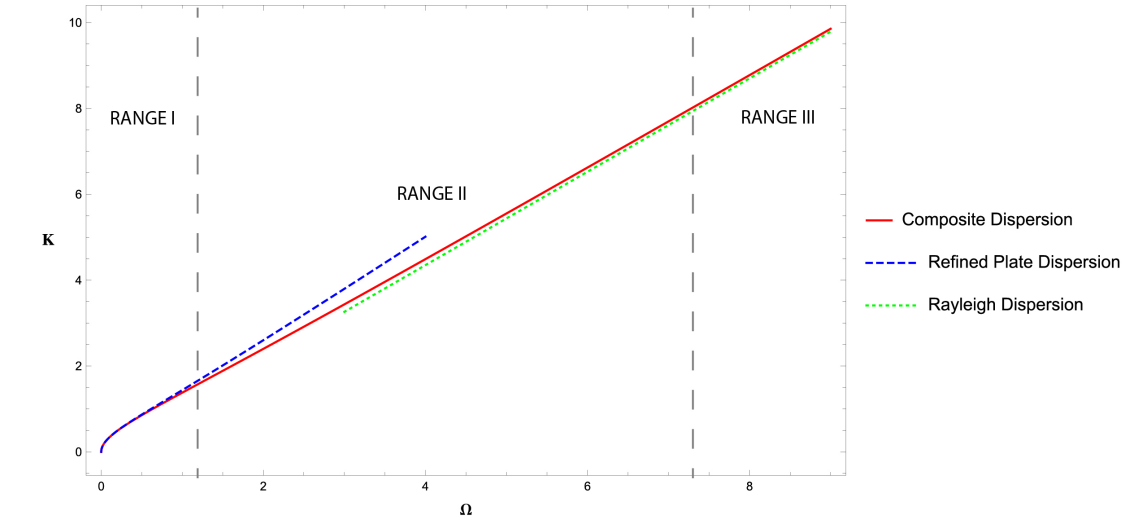

Figure 3.10. Dispersion curves for refined plate equation (3.86), composite equation (3.85), and Rayleigh wave (3.87)

According to the Figure 3.10, the behavior of the plate in different asymptotic approaches can easily be observed through dispersion curves. In the region defined as Range I, the refined plate dispersion curve and the composite dispersion curve do agree for the small values of the frequency Ω. In Range III, the Rayleigh dispersion curve and the composite dispersion curve coincide with each other, for large values of Ω.

Figure 3.11 displays the comparison of the numerical solution of Rayleigh-Lamb equation (3.111) and composite dispersion (3.85).

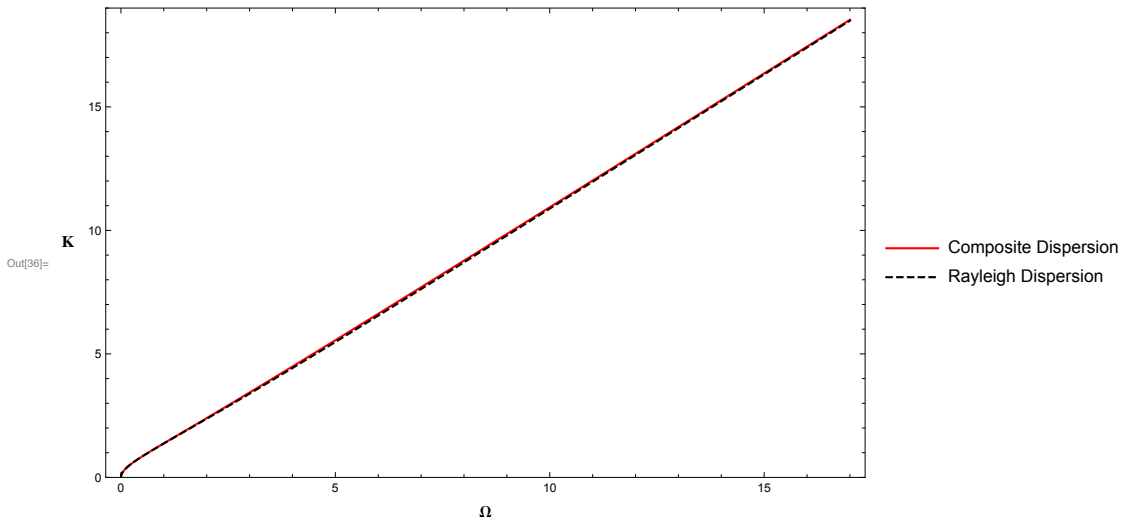

Figure 3.11. Dispersion curves for composite equation (3.85), and Rayleigh-Lamb equation (3.111)

3.9. Example

As an example, we consider the effect of the surface loads, in the form of plane time-harmonic travelling waves, for which $P = P_0 e^{i(\omega t - k_0 x)}$, where k_0 is a given by

$$k_0(\omega) = \varepsilon\sqrt{\omega} + \frac{\omega}{v_R}, \tag{3.88}$$

where small parameter ε is arbitrary.

Let us seek the solution in the form of a plane travelling wave, i.e. take $u_1 = \dfrac{ihP_oA}{\mu} e^{i(k_0 x_1 - \omega t)}$, where A is normalized amplitude.

Inserting u_1 and P into composite equation (3.76), (3.64) and (3.65) and writing in terms of dimensionless variables (3.84), we have, respectively,

$$A = \frac{K\left(\dfrac{3(1-\nu)}{4} + \dfrac{2-7\nu}{20}K^2 - \left(\dfrac{2-7\nu}{20s^2} - \dfrac{1+k_2^2}{8B}\right)\Omega^2\right)}{K^4 - \left(\dfrac{3(1-\nu)}{2} - \dfrac{7\nu-17}{10}K^2\right)\Omega^2 - \left(\dfrac{1}{s^4} + \dfrac{7\nu-17}{10s^2}\right)\Omega^4}, \tag{3.89}$$

$$A = \frac{\left(\dfrac{3(1-\nu)}{2} + \dfrac{2-7\nu}{10}K^2\right)K}{K^4 - \left(\dfrac{3(1-\nu)}{2} - \dfrac{7\nu-17}{10}K^2\right)\Omega^2}, \tag{3.90}$$

$$A = \frac{1+k_2^2}{8B}\frac{K}{K^2 - \dfrac{\Omega^2}{s^2}}. \tag{3.91}$$

Numerical data are given Figures 3.12–3.15 for $\nu = 0.25$, $v_R = 0.9194$, and $\varepsilon = 0.1$. In Figure 3.12 displacement amplitudes for composite equation (3.89), refined plate equation (3.90), and Rayleigh equation (3.91) are plotted by the red solid line, dashed blue line, and dotted green line, respectively. It is observed from Figure 3.12, the composite equation coincides with the plate limit for the small values of Ω and the Rayleigh limit for the large values of Ω.

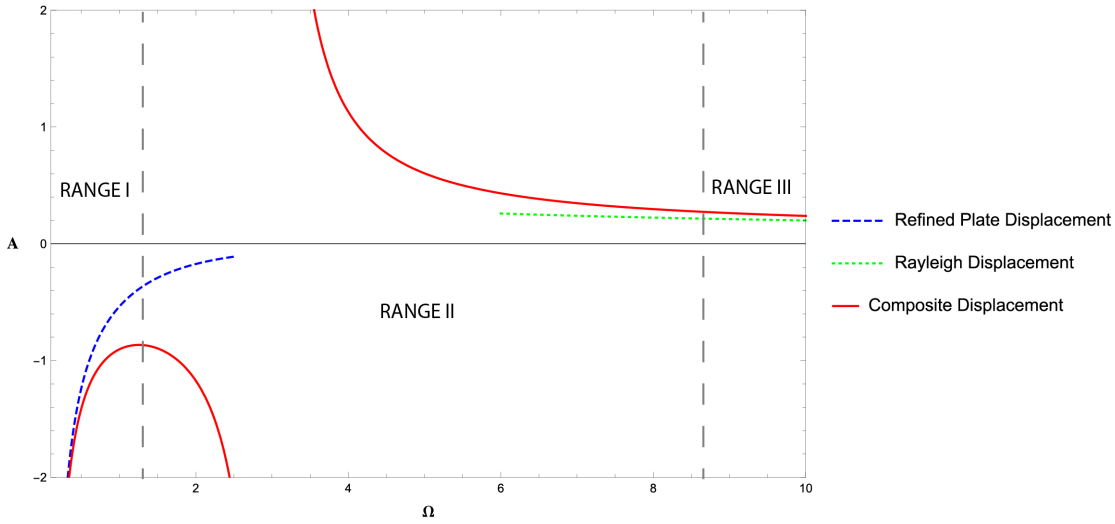

Figure 3.12. Displacement amplitude for composite equation (3.89), refined plate equation (3.90), and Rayleigh wave equation (3.91)

Since composite displacement has a singularity in Range II, the displacement curve appears in Figure 3.12 as two parts. In Range I, the refined plate displacement curve and the composite displacement curve agree, as expected, for small values of Ω. Rayleigh displacement curve and composite displacement curve matched the expectations for large values of Ω in Range III. It is also possible to make similar comparison by adding the exact solution to Figure 3.12. The exact solution is added to Range I in Figure 3.12 and the graph in Figure 3.13 is obtained. Displacement amplitudes for composite equation (3.89), exact solution (3.114), refined plate equation (3.90) and Rayleigh wave equation (3.91) are plotted by red solid, black solid, dashed blue, and dotted green lines, respectively.

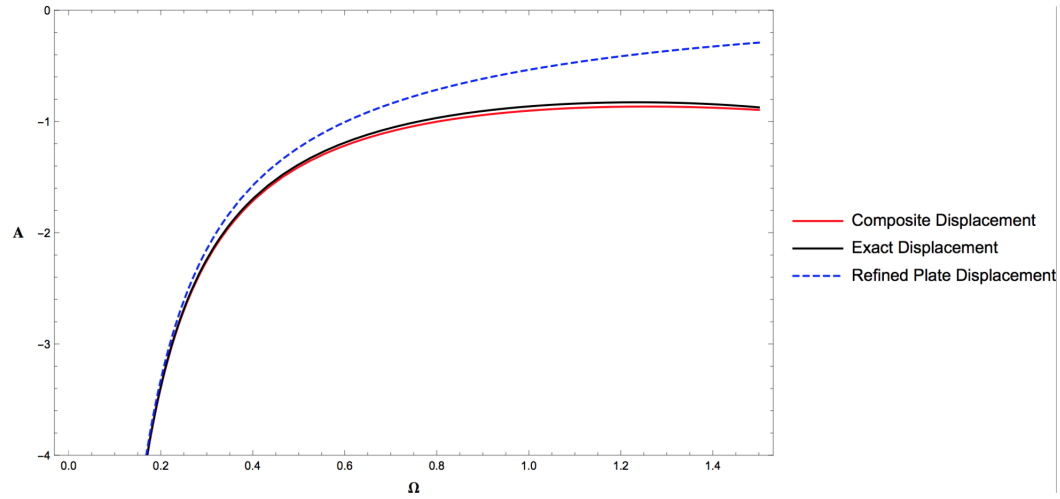

Figure 3.13. Displacement amplitude for refined plate equation (3.90), composite equation (3.89), and exact solution (3.114)

Figure 3.13 shows that the composite displacement curve is consistent not only with the long-wave low-frequency limit, but also with the exact displacement curve for small values of Ω.

Similarly, the exact solution was added to Range III in Figure 3.12 to obtain the graph in Figure 3.14. Displacement amplitudes for composite equation (3.89), exact solution (3.114), refined plate equation (3.90) and Rayleigh wave equation (3.91) are plotted by red solid, black solid, dashed blue, and dotted green lines, respectively. It is clear that composite displacement curve does also match with the exact displacement curve in short-wave high-frequency limit case.

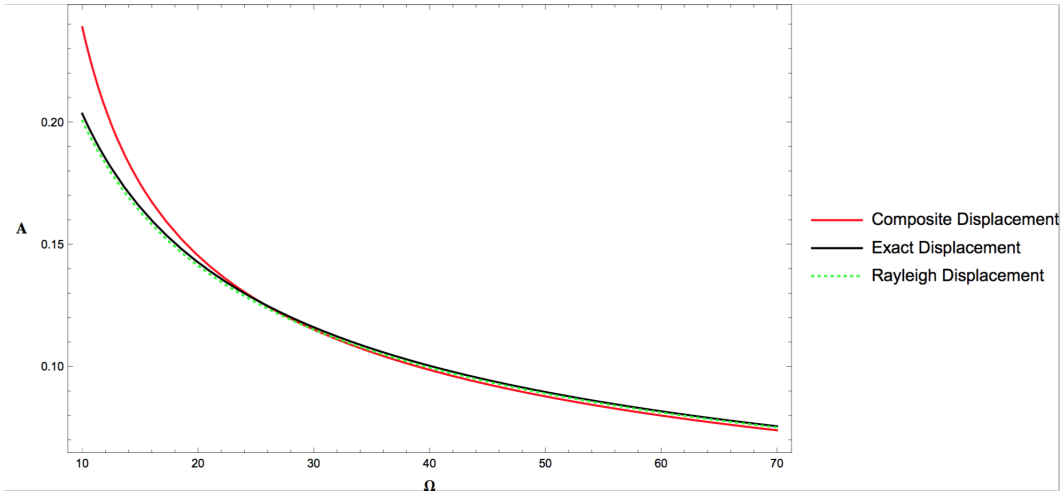

Figure 3.14. Displacement amplitude for Rayleigh wave (3.91),composite equation (3.89), and exact solution (3.114)

It is also possible to compare exact solution and composite solution directly.

In Figure 3.15 displacement amplitudes for composite equation (3.89) and exact solution (3.114) are plotted by red solid line and black solid line, respectively. In Range I and Range III the composite displacement curve and exact displacement curve are matching as expected. With this graph, it is also shown that exact solution has a singularity like exact solution in Range II.

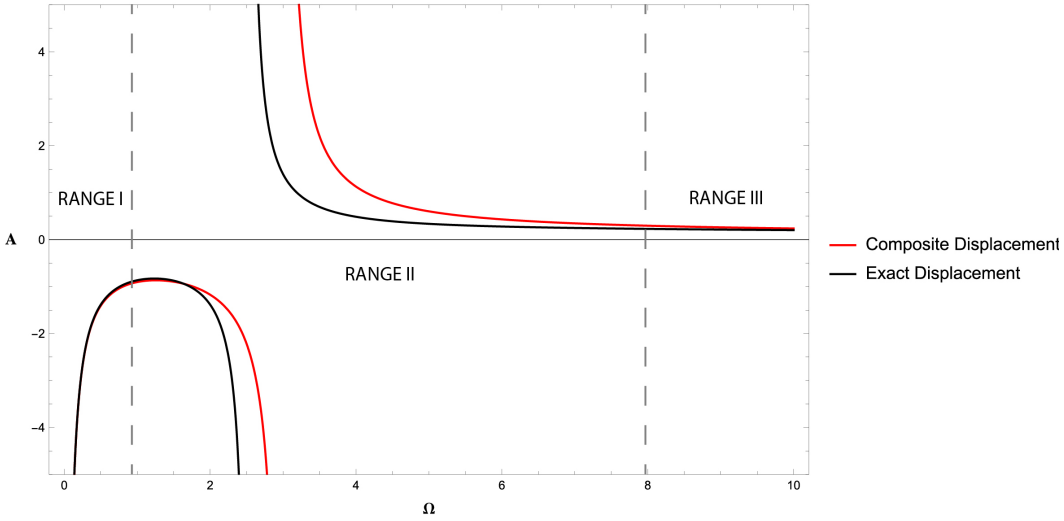

Figure 3.15. Displacement amplitude for composite equation (3.89), exact solution (3.114)

3.10. Section Summary

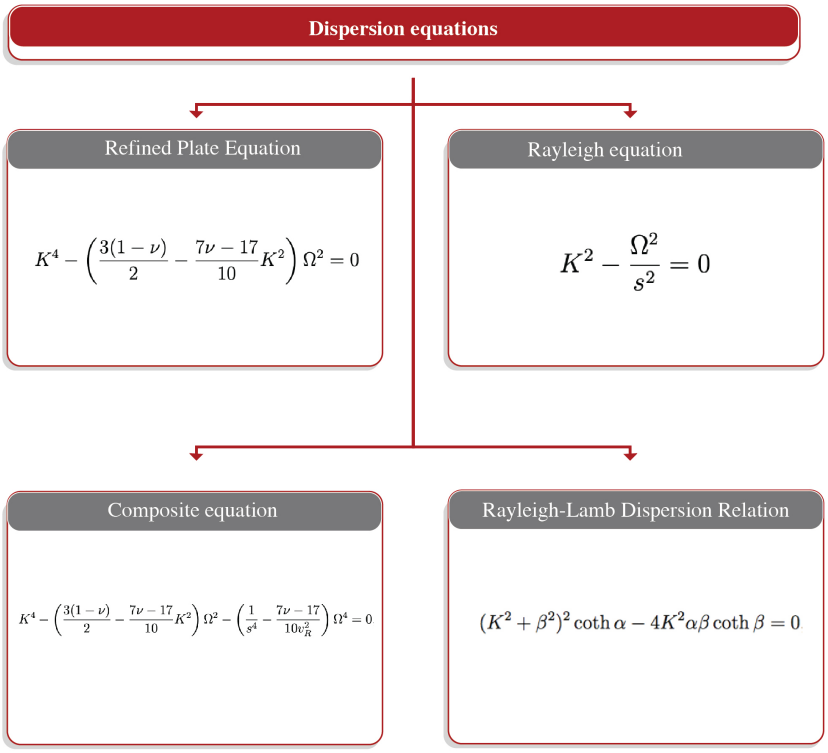

Figure 3.16. Dispersion Equations

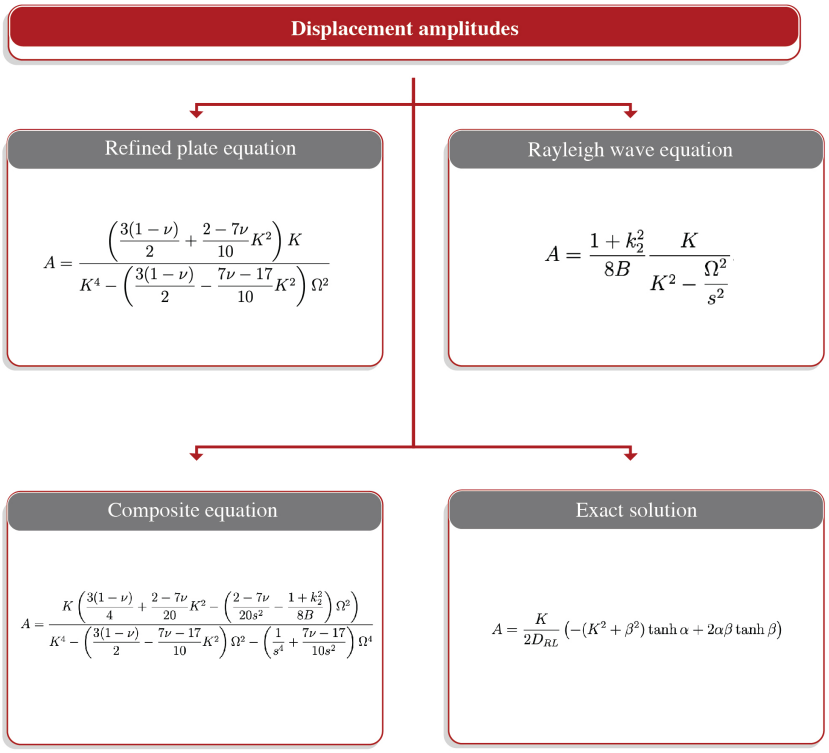

Figure 3.17. Displacement Amplitudes

3.11. APPENDIX

3.11.1. Exact solution of plane time-harmonic problem for vertical displacement

The governing equations in plane elasticity are given by (2.27),in terms of wave potentials $\varphi(x_1, x_3, t)$ and $\psi(x_1, x_3, t)$. Consider a layer $-\infty \leq x_1 \leq \infty$, $-h \leq x_3 \leq h$ as given in Figure 3.1 with the boundary conditions on its faces $x_3 = \pm h$ given by

$$\sigma_{31}|_{x_3=\pm h} = 0 \tag{3.92}$$

$$\sigma_{33}|_{x_3=\pm h} = \pm\frac{P}{2}. \tag{3.93}$$

Using (2.4), (3.92), (3.93) and taking $P = P_0 e^{kx_1-\omega t}$we have

$$\sigma_{31}|_{x_3=\pm h} = \mu\left(\frac{\partial^2\psi}{\partial x_1^2} - \frac{\partial^2\psi}{\partial x_3^2} + 2\frac{\partial^2\varphi}{\partial x_1\partial x_3}\right) = 0, \tag{3.94}$$

$$\sigma_{33}|_{x_3=\pm h} = \frac{\mu}{\chi^2}\left(\frac{\nu}{1-\nu}\frac{\partial^2\varphi}{\partial x_1^2} + \frac{\partial^2\varphi}{\partial x_3^2} + 2\chi^2\frac{\partial^2\psi}{\partial x_1\partial x_3}\right) = \pm\frac{P_0}{2}e^{i(kx_1-\omega t)}. \tag{3.95}$$

where $\chi = c_2/c_1$. We may write boundary conditions given above in terms of dimensionless variables (4.6)

$$\sigma_{31}|_{\zeta=\pm 1} = \frac{\mu}{h}\left(\frac{\partial^2\psi}{\partial\xi_1^2} - \frac{\partial^2\psi}{\partial\zeta^2} + 2\frac{\partial^2\varphi}{\partial\xi_1\partial\zeta}\right) = 0, \tag{3.96}$$

$$\sigma_{33}|_{\zeta=\pm 1} = \frac{\mu}{h\chi^2}\left(\frac{\nu}{1-\nu}\frac{\partial^2\varphi}{\partial\xi_1^2} + \frac{\partial^2\varphi}{\partial\zeta^2} + 2\chi^2\frac{\partial^2\psi}{\partial\xi_1\partial\zeta}\right) = \pm\frac{P_0}{2}e^{i(K\xi_1-\Omega\tau)} \tag{3.97}$$

The solution to the formulated problem for the vertical displacement at the faces, given by

$$u_3 = \left.\frac{\partial\varphi}{\partial x_3} + \frac{\partial\psi}{\partial x_1}\right|_{x_3=\pm h}. \tag{3.98}$$

We may rewrite (3.98) in terms of dimensionless variables(4.6) as

$$u_3 = \frac{1}{h}\left.\left(\frac{\partial\varphi}{\partial\zeta} + \frac{\partial\psi}{\partial\xi_1}\right)\right|_{\zeta=\pm h}. \tag{3.99}$$

We seek the plane travelling wave solution in the form (2.30). In this case we study antisymmetric modes, so we the take wave potentials in the form

$$\begin{aligned}\psi(\xi_1,\zeta,\tau) &= C\sinh(\alpha\zeta)e^{i(K\xi_1-\Omega\tau)},\\ \phi(\xi_1,\zeta,\tau) &= D\cosh(\beta\zeta)e^{i(K\xi_1-\Omega\tau)}.\end{aligned} \tag{3.100}$$

Inserting (3.100) into (3.96) and taking $\zeta=-1$ we get

$$\sigma_{31}|_{\zeta=-1} = \frac{E}{2(1+\nu)h^2}\left(-2iK\alpha\cosh(\alpha)C+\left(K^2-\beta^2\right)\cosh(\beta)D\right)e^{i(K\xi_1-\Omega\tau)}=0. \tag{3.101}$$

From (4.29) we get following equation with unknown parameters C and D

$$\left(-2iK\alpha\cosh(\alpha)\right)C+\left(K^2+\beta^2\right)D=0. \tag{3.102}$$

Now we use boundary condition for σ_{33} at $\zeta=-1$, inserting (3.100) into (3.97) and taking $\zeta=-1$ we get

$$\sigma_{33}|_{\zeta=-1} = \frac{\mu}{h^2\chi^2}\left(\left(\frac{-\nu}{1-\nu}K^2+\alpha^2\right)\sinh\alpha C - i\frac{2\nu-1}{1-\nu}A\beta\sinh\beta D\right)e^{i(K\xi_1-\Omega\tau)} \tag{3.103}$$

$$= -\frac{P_0}{2}e^{i(K\xi_1-\Omega\tau)}$$

From (3.103) we get

$$\left(-\frac{\nu}{1-\nu}K^2+\alpha^2\right)\sinh\alpha C - i\frac{2\nu-1}{1-\nu}K\beta\sinh\beta D = -\frac{P_0h^2\chi^2}{2\mu}. \tag{3.104}$$

Solving (3.102) and (3.104) we get,

$$D = -i\frac{P_0h^2}{2\mu}\frac{1}{\frac{(2K^2-\Omega^2)^2}{2\alpha K}\tanh\alpha\cosh\beta-2K\beta\sinh\beta} \tag{3.105}$$

and

$$C = -\frac{(K^2+\beta^2)P_0h^2}{4\mu K\alpha\cosh\alpha}\frac{1}{\frac{(2K^2-\Omega^2)^2}{2\alpha K}\tanh\alpha\cosh\beta-2K\beta\sinh\beta} \tag{3.106}$$

Substituting (3.106) and (3.105) into (3.100) and using (3.99), vertical displacement takes the form $u_3 = A\dfrac{hP_0}{\mu}e^{i(kx-\omega t)}$ with

$$A = -\frac{\alpha\Omega^2}{D_{RL}}, \tag{3.107}$$

and the Rayleigh-Lamb denominator D_{RL} written as

$$D_{RL}(K,\Omega) = (K^2+\beta^2)^2 \tanh\alpha - 4K^2\alpha\beta\tanh\beta, \tag{3.108}$$

with Ω and K defined by (2.29).

The long-wave low-frequency expansion of formula (3.107) at $\Omega \ll 1$ and $K \ll 1$ reads as

$$A = \frac{3(1-\nu)}{4}\frac{1}{K^4 - \dfrac{4}{5}K^6 - \dfrac{3(1-\nu)}{2}\Omega^2 - \dfrac{1+\nu}{2}K^2\Omega^2 + \cdots}. \tag{3.109}$$

At leading order, we have for the Rayleigh wave contribution at $K \sim \Omega \gg 1$, and $|\Omega/K - v_R| \ll 1$,

$$A = \frac{1}{4K}\frac{v_R^2\sqrt{1-\chi^2 v_R^2}}{R'(v_R)(c^2-v_R^2)}. \tag{3.110}$$

with $c = \Omega/K$, and the Rayleigh denominator given by

$$R(c) = (2-c^2)^2 - 4\sqrt{1-\chi^2c^2}\sqrt{1-c^2} \tag{3.111}$$

and prime denoting a differentiation with respect to the argument of the Rayleigh denominator.

3.11.2. Exact solution of plane time-harmonic problem for horizontal displacement

The governing equations in plane elasticity are given by (2.27),in terms of wave potentials $\varphi(x_1, x_3, t)$ and $\psi(x_1, x_3, t)$. Consider a layer $-\infty \le x_1 \le \infty$, $-h \le x_3 \le h$ as given in Figure 3.1 with the boundary conditions on its faces $x_3 = \pm h$ given by (3.92) and (3.93). The solution to the formulated problem for the horizontal

displacement at the faces is given by

$$u_1 = \left(\frac{\partial \varphi}{\partial x_1} - \frac{\partial \psi}{\partial x_3} \right) \Bigg|_{x_3 = \pm h}. \tag{3.112}$$

We may write (4.26) in terms of dimensionless variables (4.6) as follows

$$u_1 = \frac{1}{h} \left(\frac{\partial \varphi}{\partial x_1} - \frac{\partial \psi}{\partial x_3} \right) \Bigg|_{x_3 = \pm h}. \tag{3.113}$$

Using equations (3.100)-(3.106) in (3.113), the horizontal displacement component takes the form $u_1 = \dfrac{ihP_0A}{\mu} e^{\mathrm{i}(kx_1 - \omega t)}$ with

$$A = \frac{K}{2D_{RL}} \left(-(K^2 + \beta^2) \tanh \alpha + 2\alpha\beta \tanh \beta \right) \tag{3.114}$$

where α, β and Rayleigh–Lamb dispersion relation are given by (2.32) and (3.111), respectively.

4. A COMPOSITE HYPERBOLIC EQUATION FOR PLATE EXTENSION

It is well known that the 2D hyperbolic theory of plane stress, e.g. see [1], may be treated as the leading order long-wave, low- frequency approximation of the 3D equations in linear elasticity for plate extension. A drawback of this theory is that it distorts the longitudinal wave speed. As a result, a singularly perturbed hyperbolic system arising at next order, cf. [2], supports a dispersive longitudinal wave front, sometimes called quasi-front, corresponding to the wave-front predicted from the degenerated problem. However, as might be expected, neither conventional nor refined plane stress approximations are suited for modeling high-frequency, short-wave behavior. The aforementioned quasi–fronts are also observed for thin elastic rods and shells and have been tackled since long ago using both heuristic and asymptotic arguments, e.g. see [1–10] and references therein. In this Section, we attempt to develop a composite wave model for plate extension supporting not only the long–wave, low–frequency limit associated with the quasi-front, but also the short-wave, high-frequency limit involving surface waves. The latter is incorporated through the specialized formulation for the Rayleigh wave, see [11] and references therein, which includes, in particular, an explicit hyperbolic equation on the surface. There are obvious similarities between proposed composite equation and governing equations established in previous sections. The proposed formulation, as a number of composite models, e.g. see [12,13] for further detail, is not uniformly valid. However, we may expect only qualitative coincide over the intermediate range, where a typical wave length is of order plate thickness. Analogous composite wave formulations for plate bending have recently been established in [14]. Earlier, known composite dynamic theories for thin elastic structures, e.g. see [15], operated with ad hoc short-wave limits. We also mention composite models for periodic media in [16] demonstrating, again, similarity in asymptotic procedures for thin and periodic wave guides previously noted in [17]. The geometric setup considered in this section corresponds to a thin elastic strip loaded by shear stresses along its faces. A fourth-order inhomogeneous hyperbolic equation is derived. It is worth mentioning that its right-hand side contains a pseudo-differential operator acting on the prescribed

load. The dispersion curve and also the displacement amplitude induced by surface stresses in the form of a travelling harmonic wave predicted from this equation are compared with those calculated from the related plane strain problem.

4.1. Statement of the Problem

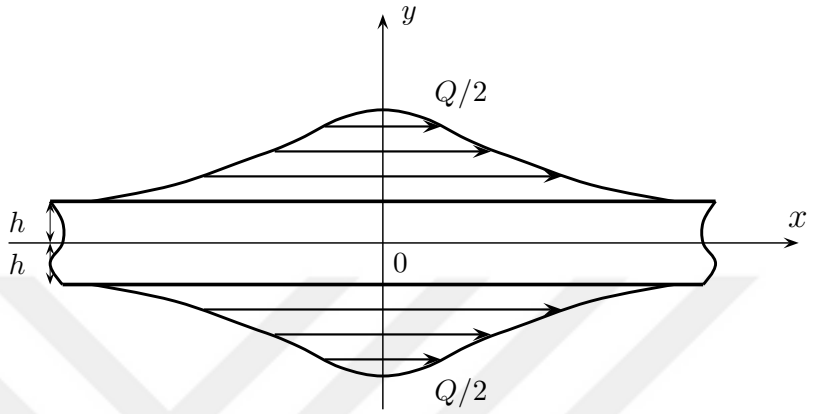

Figure 4.1. Geometrical setup of the problem.

Our concern in this section is the extension of an infinite elastic strip of thickness $2h$ ($-\infty < x < \infty, \quad -h \leq y \leq h$) subjected to symmetric tangential loads of $\pm Q/2$ at its faces $y = \pm h$, see Figure 4.1.

Let us first express the governing equation in the refined asymptotic 2D theory for plate extension written as, see [26],

$$\frac{2Eh}{1-\nu^2}\frac{\partial^2 u_1}{\partial x^2} - 2\rho h\frac{\partial^2 u_1}{\partial t^2} + 2\rho h^3\frac{\nu^2}{3(1-\nu)^2 c_3^2}\frac{\partial^4 u_1}{\partial t^4} = -Q \tag{4.1}$$

Multiplying (4.1) by $\dfrac{1-\nu^2}{2Eh}$ we get

$$\frac{\partial^2 u_1}{\partial x^2} - \frac{1}{c_3^2}\frac{\partial^2 u_1}{\partial t^2} + \frac{\nu^2 h^2}{3(1-\nu)^2 c_3^4}\frac{\partial^4 u_1}{\partial t^4} = -\frac{(1-\nu)^2}{Eh}Q \tag{4.2}$$

containing the fourth order derivative in time, smoothing the discontinuity at the quasi-front propagating with speed $c_3 = \sqrt{\dfrac{E}{\rho(1-\nu^2)}}$, where $u(x,t)$ is the longitudinal displacement, t is time, E is Young's modulus, ρ is the density, ν is the Poisson's ratio. Equation (4.2) is the first order correction to the equation of motion in the elementary theory of plate extension.

The latter is valid over long–wave low–frequency range and short–wave high–frequency

range given by (2.34) and (2.41), respectively. We adapt the asymptotic formulation for the surface Rayleigh wave given by, see [26],

$$\frac{\partial^2 u_1}{\partial x^2} - \frac{1}{c_R^2}\frac{\partial^2 u_1}{\partial t^2} = -\frac{\rho(1+\nu)\,(1+k_2^2)\,k_2}{EB}\sqrt{-\frac{\partial^2}{\partial x^2}}Q. \tag{4.3}$$

Our aim is to derive a composite equation having both singularly perturbed hyperbolic equation (4.3), and as local long–wave low frequency and short wave–high frequency limits.

4.2. Construction of Composite Equation

First we differentiate (4.3) twice in time having

$$\frac{\partial^4 u_1}{\partial x^2 \partial t^2} - \frac{1}{c_R^2}\frac{\partial^4 u_1}{\partial t^4} = -\frac{\rho(1+\nu)\,(1+k_2^2)\,k_2}{EB}\sqrt{-\frac{\partial^2}{\partial x^2}}\frac{\partial^2 Q}{\partial t^2}. \tag{4.4}$$

We now combine (4.2) and (4.4) in the following way to suggest a composite equation: we keep the second order spatial derivative on the left hand side of both equations; then qe write the fourth order time derivative in equation (4.2) in terms of second order spatial and time derivatives. We then multiply the second term on the left hand side of equation (4.4) as well as its right hand side by Γ and combine the obtained forms to get

$$\begin{aligned}\frac{\partial^2 u_1}{\partial x^2} - \frac{1}{c_3^2}\frac{\partial^2 u_1}{\partial t^2} + \Gamma h^2 \frac{\partial^2}{\partial t^2}\left(\frac{\partial^2 u_1}{\partial x^2} - \frac{1}{c_R^2}\frac{\partial^2 u_1}{\partial t^2}\right) = \\ = -\frac{\rho(1+\nu)}{E}\left(\frac{1-\nu}{h} - \Gamma h^2 \frac{(1+k_2^2)\,k_2}{B}\sqrt{-\frac{\partial^2}{\partial x^2}}\frac{\partial^2}{\partial t^2}\right)Q.\end{aligned} \tag{4.5}$$

Next, we need rescale the spatial and time variables as

$$\xi = \frac{x}{L}, \qquad \tau = \frac{c_3 t}{L}, \tag{4.6}$$

where $c_3 = \sqrt{\dfrac{E}{\rho\,(1-\nu^2)}}$ and assuming that $\eta = \dfrac{h}{L} \ll 1$, we get from (4.5)

$$\begin{aligned} &\frac{1}{L^2}\left(\frac{\partial^2 u_1}{\partial \xi^2} - \frac{\partial^2 u_1}{\partial \tau^2}\right) + \Gamma\eta^2 c_3^2 \frac{\partial^2}{\partial \tau^2}\left(\frac{1}{L^2}\frac{\partial^2}{\partial \xi^2} - \frac{1}{L^2}\frac{c_3^2}{c_R^2}\frac{\partial^2}{\partial \tau^2}\right) u_1 = \\ &\quad = -\frac{\rho(1+\nu)}{Eh}\left(1 - \nu + \eta^2\Gamma\frac{(1+k_2^2)\,k_2}{B}\sqrt{-\frac{\partial^2}{\partial \xi^2}}c_3^2\frac{\partial^2}{\partial \tau^2}\right) Q. \end{aligned} \tag{4.7}$$

The left hand side of the last equation, within the same truncation error, can be written as

$$\frac{\partial^2 u_1}{\partial \xi^2} - \frac{\partial^2 u_1}{\partial \tau^2} + \Gamma\eta^2 c_3^2 \frac{\partial^2}{\partial \tau^2}\left(\frac{\partial^2}{\partial \xi^2} - \frac{c_3^2}{c_R^2}\frac{\partial^2}{\partial \tau^2}\right) u_1 = 0. \tag{4.8}$$

Since, at leading order, we have $\dfrac{\partial^2 u}{\partial \xi^2} = \dfrac{\partial^2 u}{\partial \tau^2}$ we get

$$\frac{\partial^2 u_1}{\partial \xi^2} - \frac{\partial^2 u_1}{\partial \tau^2} + \Gamma\eta^2 c_3^2\left(1 - \frac{c_3^2}{c_R^2}\right)\frac{\partial^4 u_1}{\partial \tau^4} = 0. \tag{4.9}$$

Now we require (4.9) to coincide with thehomogenous part of (4.2) taking the dimensionless form

$$\frac{\partial^2 u_1}{\partial \xi^2} - \frac{\partial^2 u_1}{\partial \tau^2} + \eta^2\frac{\nu^2}{3(1-\nu)^2}\frac{\partial^4 u_1}{\partial \tau^4} = 0. \tag{4.10}$$

Comparing equations (4.9) and (4.10) we arrive at

$$\Gamma c_3^2\left(1 - \frac{c_3^2}{c_R^2}\right) = \frac{\nu^2}{3(1-\nu)^2}. \tag{4.11}$$

From (4.11), we find Γ as

$$\Gamma = \frac{\nu^2 c_R^2}{3(1-\nu)^2\,(c_R^2 - c_3^2)\,c_3^2}. \tag{4.12}$$

Thus, the sought for composite equation takes the form (4.5) with (4.12). In fact, it is constructed such as long–wave low–frequency limit coincide with equation (4.2) while at short–wave high–frequency limit for which $\eta = h/L \gg 1$ we obviously have at leading order the scaled equation (4.3).

4.3. Dispersion Analysis

Consider dispersion relations corresponding to the derived composite equation (4.5) with (4.12) and its limiting forms (4.4) and (4.2). They are given by respectively

$$k^2 - \frac{\omega^2}{c_3^2} - \frac{\nu^2 h^2}{3(1-\nu)^2 c_3^4}\omega^4 = 0, \tag{4.13}$$

$$k^2 - \frac{\omega^2}{c_R^2} = 0, \tag{4.14}$$

$$k^2 - \frac{\omega^2}{c_3^2} - \Gamma h^2 \omega^2 \left(k^2 - \frac{\omega^2}{c_R^2}\right) = 0, \tag{4.15}$$

with wavenumber k and angular frequency ω. Using dimensionless wave number and angular frequency

$$K = kh \qquad \Omega = \frac{\omega h}{c_2} \tag{4.16}$$

in (4.13), (4.14) and (4.15) we get

$$K^2 - \frac{c_2^2}{c_3^2}\Omega^2 - \frac{\nu^2}{3(1-\nu)^2}\frac{c_2^4}{c_3^4}\Omega^4 = 0, \tag{4.17}$$

$$K^2 - \frac{c_2^2}{c_R^2}\Omega^2 = 0, \tag{4.18}$$

$$K^2 - \frac{c_2^2}{c_3^2}\Omega^2 - \Gamma c_2^2 \Omega^2 \left(K^2 - \frac{c_2^2}{c_R^2}\Omega^2\right) = 0. \tag{4.19}$$

4.4. Numerical Results

Numerical results are demonstrated at $K(\Omega) = (1+\varepsilon)\Omega/v_R$ with $\varepsilon = 0.1$ and $\nu = 0.25$, for which $v_R = 0.9194$ in Figures 4.2 and 4.3 . Figure 4.2 displays the solutions of limiting equations (4.17) and (4.18) versus the solution of composite equation (4.19). Figure 4.3 shows the comparison of solution of the Rayleigh-Lamb equation (4.37) and composite equation (4.19).

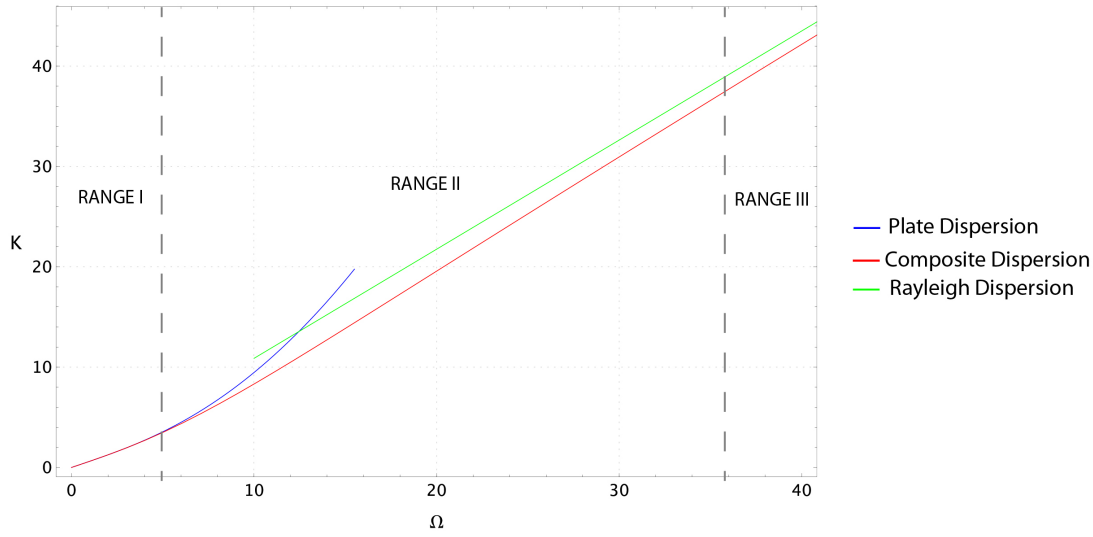

Figure 4.2. Dispersion curves for plate (4.17) (blue line), Rayleigh (4.18) (green line) and composite equation(4.19) (red line).

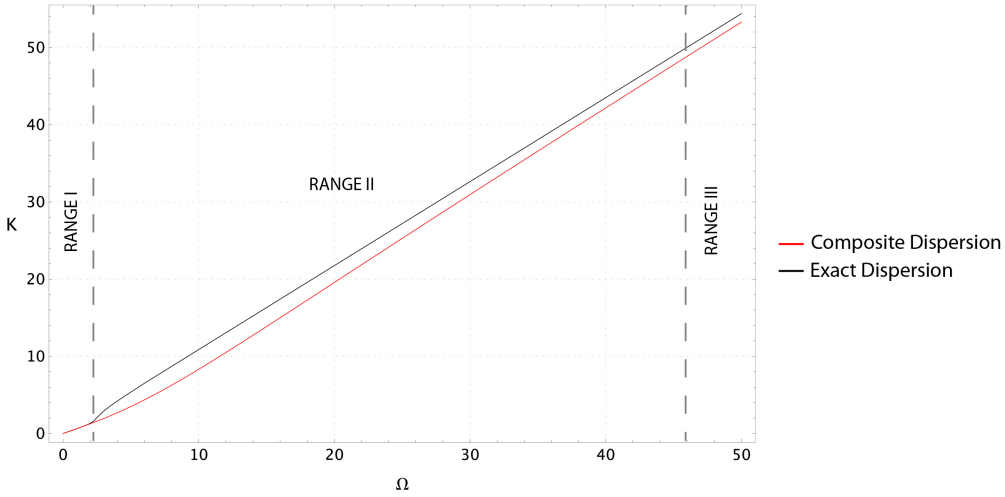

Figure 4.3. Dispersion curves for exact dispersion (4.37) (black line) and composite equation(4.19) (red line).

4.5. Exact Solution of plane time-harmonic problem

The governing equations in plane elasticity are given by (2.27), in terms of wave potentials $\varphi(x_1, x_3, t)$ and $\psi(x_1, x_3, t)$. Consider a layer $-\infty \leq x_1 \leq \infty$, $-h \leq x_3 \leq h$ as given in Figure 3.1 with the boundary conditions on its faces $x_3 = \pm h$ are given

by

$$\sigma_{31}|_{x_3=\pm h} = \pm\frac{Q}{2} \tag{4.20}$$

$$\sigma_{33}|_{x_3=\pm h} = 0. \tag{4.21}$$

Using (4.20) in (2.4) we have

$$\sigma_{31} = \frac{E}{2(1+\nu)}\left(\frac{\partial^2\psi}{\partial x^2} - \frac{\partial^2\psi}{\partial y^2} + 2\frac{\partial^2\varphi}{\partial x\partial y}\right)\Big|_{y=\pm h} = \pm\frac{Q}{2}, \tag{4.22}$$

$$\sigma_{33} = \frac{E}{2(1+\nu)\chi^2}\left(\frac{\nu}{1-\nu}\frac{\partial^2\phi}{\partial x^2} + \frac{\partial^2\phi}{\partial y^2} + 2\chi^2\frac{\partial^2\psi}{\partial x\partial y}\right)\Big|_{y=\pm h} = 0, \tag{4.23}$$

where χ is, as before, $\chi = \dfrac{c_2}{c_1}$

We may write boundary conditions (4.22) in terms of dimensionless variables as

$$\sigma_{31}|_{\zeta=\pm 1} = \frac{\mu}{h}\left(\frac{\partial^2\psi}{\partial\xi_1^2} - \frac{\partial^2\Psi}{\partial\zeta^2} + 2\frac{\partial^2\varphi}{\partial x_1\partial\zeta}\right) = \pm\frac{Q}{2}e^{i(K\xi_1-\Omega\tau)} \tag{4.24}$$

$$\sigma_{33}|_{\zeta=\pm 1} = \frac{\mu}{h\chi^2}\left(\frac{\nu}{1-\nu}\frac{\partial^2\varphi}{\partial\xi_1^2} + \frac{\partial^2\varphi}{\partial\zeta^2} + 2\chi^2\frac{\partial^2\psi}{\partial\xi_1\partial\zeta}\right) = 0. \tag{4.25}$$

The solution to the formulated problem for the horizontal displacement at the faces,

$$u_1 = \left(\frac{\partial\Phi}{\partial x} - \frac{\partial\psi}{\partial z}\right)\Big|_{y=\pm h} \tag{4.26}$$

We may write (4.26) in terms of dimensionless variables (4.6) as follows

$$u_1 = \frac{1}{h}\left(\frac{\partial\Phi}{\partial\zeta} + \frac{\partial\Psi}{\partial\xi_1}\right)\Big|_{\zeta=\pm h}. \tag{4.27}$$

We seek the plane travelling wave solution in the form (2.30). In this case we study symmetric modes, so we will take wave potentials as follows

$$\begin{aligned}\phi(\xi_1,\zeta,\tau) &= E\sinh\alpha\zeta e^{i(\Omega\tau-K\xi)},\\ \psi(\xi_1,\zeta,\tau) &= F\cosh\alpha\zeta e^{i(\Omega\tau-K\xi)},\end{aligned} \tag{4.28}$$

with α and β given by (2.32). Inserting (4.28) into (5.24) and (5.25), and taking $\zeta = -1$ we get

$$\sigma_{31}|_{\zeta=-1} = \frac{\mu}{h}\left(\left(2K^2 - \Omega^2\right)\sinh\beta F + 2iK\alpha\sinh\alpha E\right) = -Q. \tag{4.29}$$

$$\left(2K^2 - \Omega^2\right)\sinh\beta F + 2iK\alpha\sinh\alpha F = -\frac{Qh}{\mu}. \tag{4.30}$$

Now we use boundary condition for σ_{33} at $\zeta = -1$, inserting (4.28) into (5.25) and taking $\zeta = -1$ we get

$$\sigma_{33}|_{\zeta=-1} = \frac{\mu}{h^2\chi^2}\left(\left(-\frac{\nu}{1-\nu}K^2 + \alpha^2\right)\cosh\alpha E - 2\chi^2 iK\beta\cosh\beta F\right) = 0, \tag{4.31}$$

$$\left(2K^2 - \Omega^2\right)\cosh\alpha E - 2iK\beta\cosh\beta F = 0. \tag{4.32}$$

Solving (4.30) and (4.32) we get,

$$E = -\frac{Qh}{\mu}\frac{(2K^2 - \Omega^2)\cosh\alpha}{(2K^2 - \Omega^2)^2\sinh\beta\cosh\alpha - 4K^2\alpha\beta\sinh\alpha\cosh\beta} \tag{4.33}$$

and

$$F = -\frac{Qh}{\mu}\frac{2iK\alpha\beta\cosh\beta}{(2K^2 - \Omega^2)^2\sinh\beta\cosh\alpha - 4K^2\alpha\beta\sinh\alpha\cosh\beta} \tag{4.34}$$

Substituting (4.33) and (4.34) into (4.28), horizontal displacement (4.27) takes the form

$$u_1 = \frac{AhQ}{\mu}e^{i(kx-\omega t)} \tag{4.35}$$

with

$$A = -\frac{\Omega^2\beta}{D_{RL}(K,\Omega)}, \tag{4.36}$$

where the Rayleigh–Lamb denominator for symmetric modes is written as

$$D_{RL}(K,\Omega) = (2K^2 - \Omega^2)^2\coth\alpha - 4K^2\alpha\beta\coth\beta, \tag{4.37}$$

with Ω and K defined in Section 3.2. The long-wave low-frequency expansion of formula (4.36) at $\Omega \ll 1$ and $K \ll 1$ takes the form

$$A = -\frac{1-\nu}{2} \frac{1}{K^2 - \dfrac{\nu^2}{12}\Omega^4 - \dfrac{2}{1-\nu}\Omega^2 + \ldots}. \tag{4.38}$$

At leading order, we have for the Rayleigh wave contribution at $K \sim \Omega \gg 1$, and $|\frac{\Omega}{K} - v_R| \ll 1$

$$A = \frac{1}{4K} \frac{v_R^2 \sqrt{1-c^2}}{R'(v_R)\,(c^2 - v_R^2)}, \tag{4.39}$$

where $c = \Omega/K$, and the Rayleigh denominator is given by

$$R(c) = \left(2 - c^2\right)^2 - 4\sqrt{1-\xi^2 c^2}\sqrt{1-c^2}, \tag{4.40}$$

with prime denoting a differentiation with respect to the argument of the Rayleigh denominator.

4.6. Example of Forced Problem

Consider harmonic surface load as $Q = Q_0 e^{i(kx-\omega t)}$, where k and ω are wavenumber and frequency, respectively, taking the horizontal displacement as $u = \dfrac{AhQ_0}{\mu} e^{i(kx-\omega t)}$, where A is dimensionless amplitude and μ is Lamé constant. Inserting u and Q into (4.2), (4.3) and (4.7)

$$A = \frac{1-\nu}{K^2 - \dfrac{c_2^2}{c_3^2}\Omega^2 - \dfrac{\nu^2}{3(1-\nu)^2}\dfrac{c_2^4}{c_3^4}\Omega^4}, \tag{4.41}$$

$$A = \frac{(1+k_2^2)\,k_2}{2B} \frac{K}{K^2 - \dfrac{c_2^2}{c_R^2}\Omega^2}, \tag{4.42}$$

$$A = \frac{1}{2} \frac{(1-\nu) + \Gamma \dfrac{(1-k_2^2)\,k_2}{B} K\Omega^2}{K^2 - \dfrac{c_2^2}{c_3^2}\Omega^2 - \Gamma c_3^2 \Omega^2 \left(K^2 - \dfrac{c_2^2}{c_R^2}\Omega^2\right)}, \tag{4.43}$$

where $\Gamma = \gamma c_2^2$. In the following figures, numerical data are demonstrated at $K(\Omega) = (1+\varepsilon)\Omega/v_R$ with $\varepsilon = 0.1$. As above, $\nu = 0.25$ and $v_R = 0.9194$. Figure (4.4) displays

the solutions of limiting equations (4.41) and (4.42) versus the solution of composite equation (4.43). Since our main interest is to derive composite asymptotic equation that is valid for long–wave low–frequency and short–wave high–frequency limits, we only need to consider the coherence between displacement curves in the Range I and Range III in following graphs.

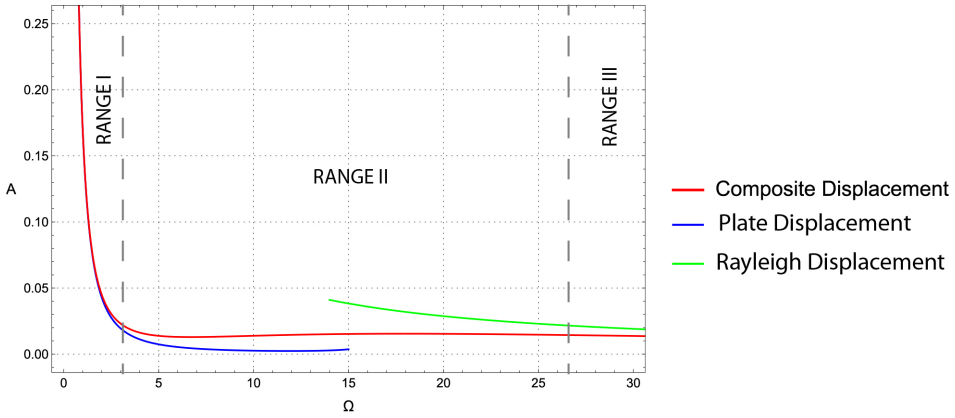

Figure 4.4. The displacement amplitudes for plate displacement (4.41) (blue line), composite displacement(4.43) (red line) and Rayleigh displacement (4.42) (green line).

In Figure (4.4) displacement curve (4.41), composite displacement curve (4.43) and Rayleigh displacement curve (4.42) are plotted by blue, red and green lines, respectively. Over long–wave low-frequency range, Range I, the graph shows that plate displacement and composite displacement are in good agreement. According to the graph it is also possible to say that composite displacement curve approaches to Rayleigh limit over short–wave high–frequency range, Range III.

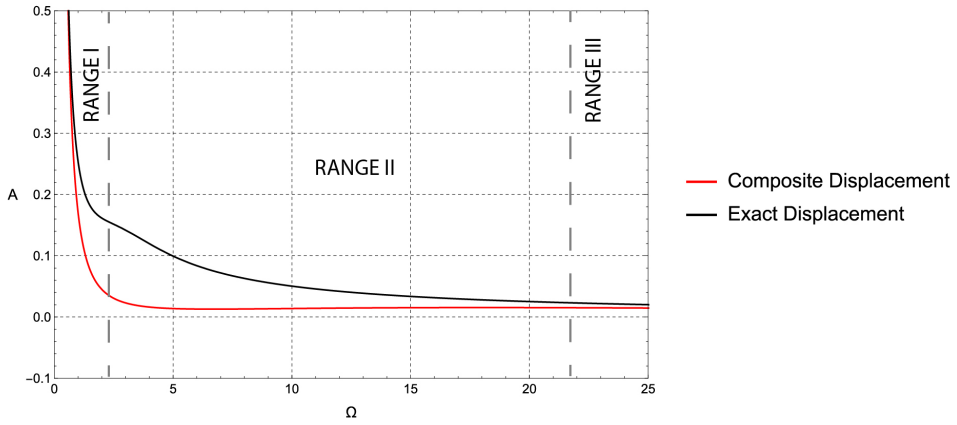

Figure 4.5. Comparison of exact solution (4.38) (black line) and composite displacement(4.43) (red line).

Figure (4.5) illustrates the exact solution (4.38) and composite displacement curve (4.43) by black and red solid lines, respectively. It is clearly observed that the exact and composite displacements coincide in Range I and Range III, as expected. Thus, it is possible to say that composite equation works properly in both limit case, but intermediate range.

4.7. Section Summary

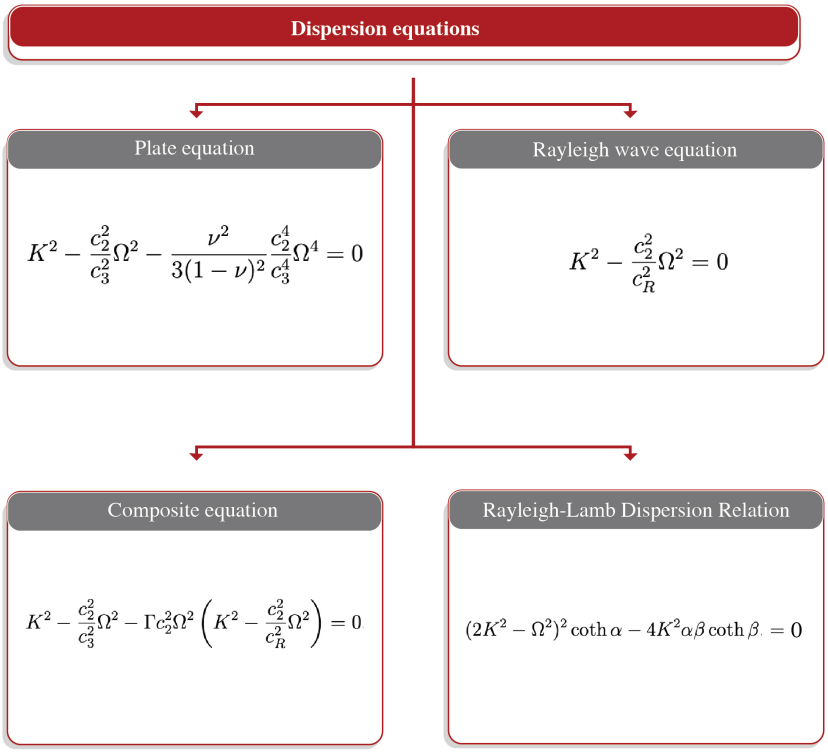

Figure 4.6. Dispersion Equations

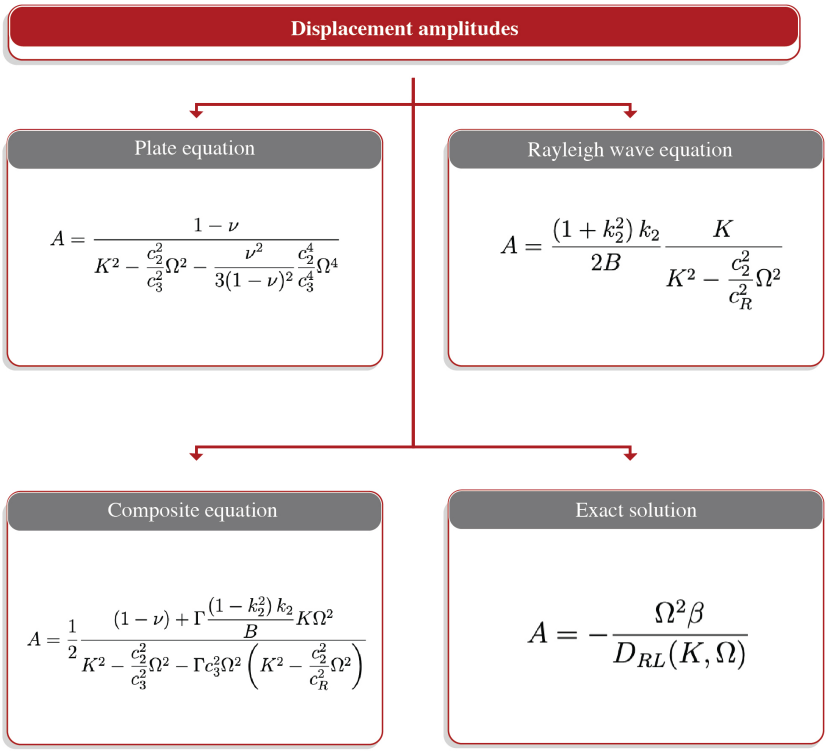

Figure 4.7. Displacement Amplitudes

5. Conclusion

This thesis is mainly concerned about the dynamics of thin elastic bodies under given external load. To this end three different problem studied with different loading, and different composite equations obtained from different cases. The main idea is combine long–wave low–frequency limit terms and short–wave high–frequency limit terms in one composite equation, and it must be valid at two limit cases. To show the validity of obtained composite equations, we will often compare numerical and asymptotic solutions throughout this thesis.

In Section 2, at first problem, aimed at deriving a composite model for horizontal displacement that is satisfies plate and Rayleigh limit asymptotically. The composite equation that obtained with the help of dispersion analysis. The deriving of the asymptotically approximate equations requires appropriate rescaling of the spatial and time variables as well as particle displacements and pressure increment, so the first Section, with all its positive results, is a guide to the problems done in latter sections. Second problem discussed is establish a composite wave equation, for thin plate under symmetric loading, in terms of horizontal displacement. We followed similar approach done for vertical, but this time worked with symmetric modes for plate. Dispersion alaysis and comparison of displacement amplitudes also done for this problem. Consistent results obtained from comparisons with numerical results once again proved the accuracy of the chosen asymptotic approach.

In third problem discussed in this thesis, aimed to obtain composite equation for plate extension. This time all equations used in terms of horizontal displacement and studied symmetric modes of plate. A composite wave formulation obtained , having as its shortened forms the refined plate equation and the hyperbolic Rayleigh wave operator is derived. It is shown that the associated dispersion curve approximates the limiting behaviors of the fundamental symmetric Rayleigh–Lamb mode at limit cases. The acquired composite equation also demonstrates a reasonable accuracy in evaluating forced vibration amplitudes, as it follows from the comparison with the exact solution of the related plane strain problem presented in Appendix. The developed methodology may readily be extended to the 2D setup and to the analysis of non-symmetric surface loading, when along with the considered in the

paper extensional modes, bending modes, studied in [26], are also induced. Further implementation of the composite equation that obtained, especially in transient problems, appears to be of interest. Finally, we mention that various comments on peculiarities and limitations of composite wave models for plate bending made in [26], are seemingly relevant for the case of plate extension treated in the section.

It is thought that the asymptotic method used in the thesis will facilitate the industrial applications related to the subject and will solve the analytical solution deficiencies in the literature. It is also an advantage that the method can be easily adapted to different loading types. It is believed that it will be expanded to different problems and structures in the future and will find different application areas. The results obtained, contrary to the ones existing in literature, in terms of elementary functions and therefore considerably simplified the physical and mathematical analysis of the problems.

REFERENCES

[1] Euler L, 1766, *De motu vibratorio tympanorum*, Novi Commentari Acad Petropolit, vol. 10, pp. 243-260.

[2] Kirchhoff GR, 1850, *Uber das gleichgewichi und die bewegung einer elastishem scheibe*, J Fuer die Reine und Angewandte Mathematik, vol. 40, pp. 51-88.

[3] Krylov AN, 1898, *On stresses experienced by a ship in a sea way*, Trans Inst Naval Architects, vol. 40, London, pp. 197-209.

[4] Bubnov IG, 1914, *Theory of Structures of Ships*, vol. 2, St . Petersburg.

[5] Timoshenko SP & Woinowsky-Krieger S, 1959, *Theory of Plates and Shells*, 2nd edn, McGraw-Hill, New York.

[6] Hencky H, 1921, *Der spanngszustand in rechteckigen platten (Diss.)*, Z Andew Math und Mech, vol.1.

[7] Huber MT, 1929, *Probleme der Static Techish Wichtiger Orthotroper Platten*, Warsawa.

[8] Von Karman T, 1910, *Fesigkeitsprobleme in Maschinenbau*, Encycl der Math Wiss, vol. 4, pp. 348-351.

[9] Von Karman T, Ef Sechler & Donnel LH, 1932, *The strength of thin plates in compression*, Trans ASME, vol. 54, pp. 53-57.

[10] Nadai A, 1915, *Die formanderungen und die spannungen von rechteckigen elastischen platten*, Forsch a.d. Gebiete d Ingeineurwesens, Berlin, Nos. 170 and 171.

[11] Föppl A., 1944, 1951, *Vorlesungen uber technische Mechanik*, vols 1 and 2, 14th and 15th edns, Verlag R., Oldenburg, Munich.

[12] Timoshenko SP, and Gere JM, 1956, *Theory of Elastic Stability*, 2nd edn, McGraw-Hill, New York, 1961.Volmir, A.S., Flexible Plates and Shells, Gos. Izdvo Techn. Teoret. Litry, Moscow, (in Russian).

[13] Volmir AS, 1963, *Stability of Elastic Systems*, Gos Izdvo Fiz-Mat. Lit., Moscow,(in Russian).

[14] Cox HL, 1933, *Buckling of Thin Plates in Compression*, Rep. and Memor., No. 1553, 1554.

[15] Goldenveizer AL, 1968, *Methods of verifying and refining the theory of shells.* Prikl. Mat. Mekh., 32 (4), pp. 684-695.

[16] Grigolyuk EI & Selezov IT, 1973, *Reviews of Science and Technology*, Ser. Mechanics of Deformable Solids (In Russian).

[17] Goldenveizer AL, 1976, *Theory of Elastic Thin Shells*, 2nd edn. Nauka, Moscow, (In Russian).

[18] Rutten HS, 1971, *Asymptotic Approximation in the Three-Dimensional Theory of Thin and Thick Elastic Shells*, Nederlands.

[19] Kaplunov JD, Zakharov A & Prikazchikov DA , 2006, *Explicit models for elastic and piezoelastic surface waves*, IMA J. Appl. Math. 71, 768-782.

[20] Goldenveizer AL,1963, *Derivation of an approximate theory of shells by means of asymptotic integration of the equations of the theory of elasticity*, Prikl. Mat. Mekh., 27 (4), pp. 593-608.

[21] Kaplunov JD & Kossovich LY, 2004, *Asymptotic model of Rayleigh waves in the far-field zone in an elastic half-plane*, Dokl. Phys., 2004, 49, 234-236.

[22] Chadwick P, 1976, *Surface and interfacial waves of arbitrary from in isotropic elastic media*, J. Elast., 6,73-80.

[23] Kaplunov J, Nolde EV, & Prikazchikov DA,2010, *A revisit to the moving load problem using an asymptotic model for the Rayleigh wave*, Wave motion, 47(7), 440-451.

[24] Erbaş B, Kaplunov JD, Prikazchikov DA, 2012, *The Rayleigh wave field in mixed problems for a half-plane*, IMA J. Appl. Math.

[25] Erbaş B, Kaplunov JD, Prikazchikov DA & Şahin O, 2013, *On a 3D moving load problem for an elastic half plane*, Wave Motion.

[26] Kaplunov JD, Kossovich LYu & Nolde EV, 1998, *Dynamics of thin walled elastic bodies*, Academic Press, UK.

[27] Graff KF, 2012, *Wave motion in elastic solids*,Courier Corporation.

[28] Achenbach J, 2012 *Wave propagation in elastic solids* (Vol. 16). Elsevier.

[29] Awrejcewicz J, Andrianov IV & Manevitch LI, 2012 *Asymptotic approaches in nonlinear dynamics: new trends and applications* (Vol. 69), Springer Science & Business Media.

[30] Kaplunov JD & Prikazchikov DA, 2017, *Asymptotic Theory for Rayleigh and Rayleigh-Type Waves*,Advances in Applied Mechanics.

[31] Goldenveizer AL, Kaplunov JD & Nolde EV, 1993, *On Timoshenko-Reissner type theories of plates and shells*, Int. J. Solids Structures 30, 675-694.